Structural diagnostics of functional materials in action: capabilities of X-ray synchrotron techniques

Yan Zubavichus

National Research Centre «Kurchatov Institute», Moscow, Russia

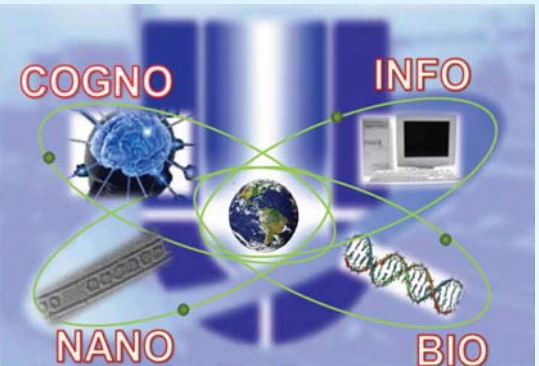

Scope of the lecture

- Introduction to synchrotron radiation (SR)
- Scheme and capabilities of the Structural Materials Science beamline at the Kurchatov SR source
- Experiments aimed at techniques development
- Examples of combined structural studies of complex materials

Synchrotron Radiation

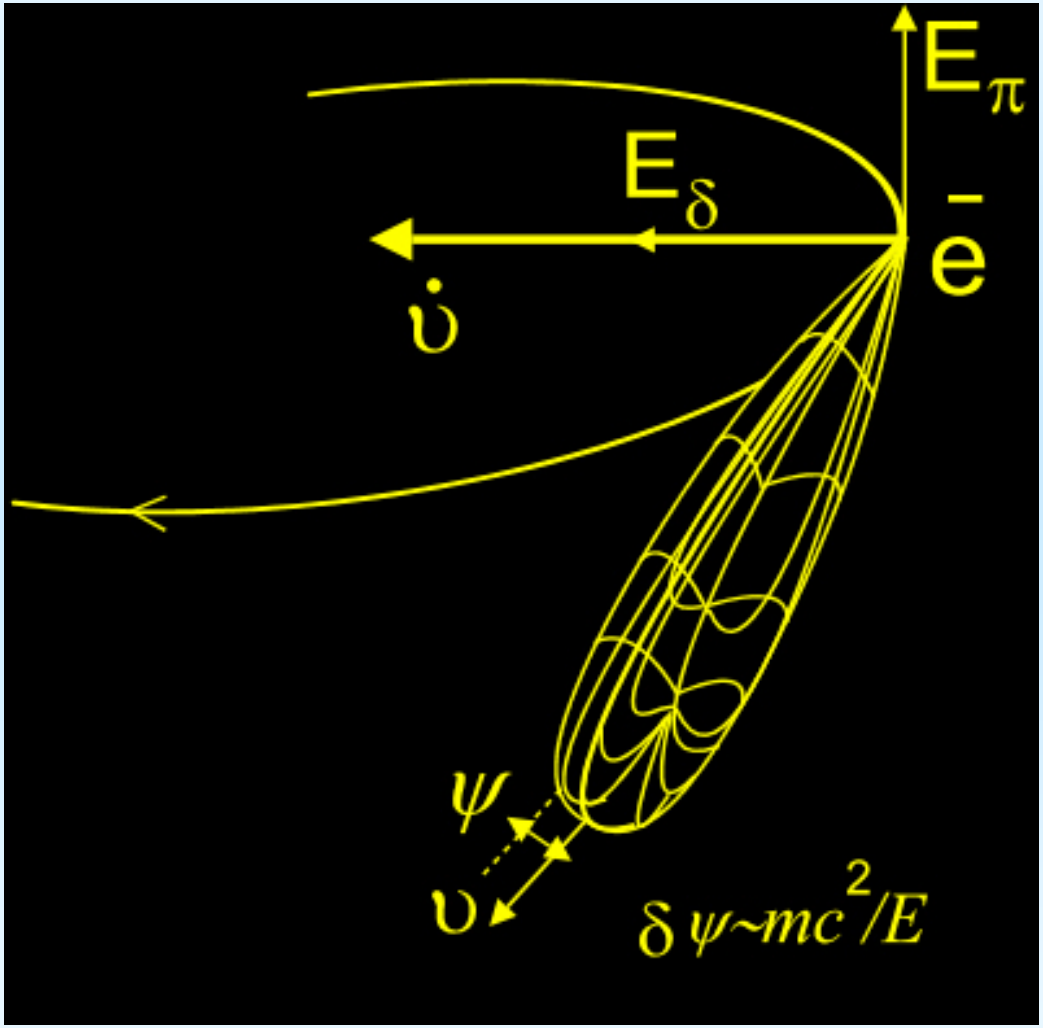

Electromagnetic radiation generated by ultrarelativistic electrons/positrons traveling along circular orbits in accelerators of light charged particles (e^-/p^+)

Advantages compared to standard X-ray sources

- Intensity/Brightness higher by 6-10 orders of magnitude
- Continuum spectrum from IR to hard X-rays
- High natural collimation
- Tunable polarization
- Partial coherence

Synchrotron X-ray techniques

Spectroscopy

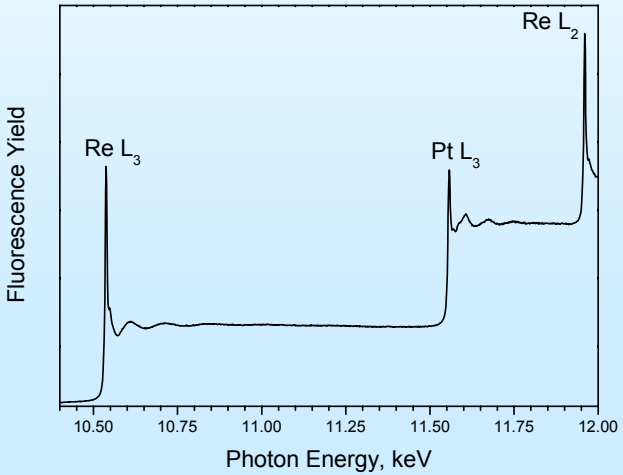

Diffraction

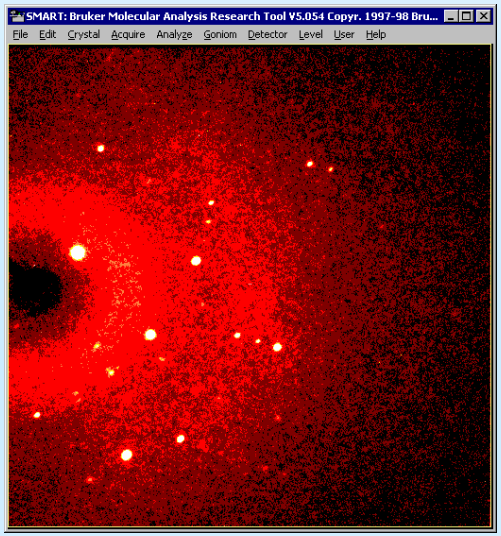

Imaging

Mixed and combined techniques (anomalous scattering, microspectroscopy, etc.)

The World Synchrotron Community
MAX
BESSY
VEPP
Новосибирск
DORIS & PETRA
ELSA
ANKA
SRS
Diamond
SLS
ELETTRA
Soleil
ESRF
Гренобль
ALBA
Барселона
DAFNE
Фраскати
Москва
SIBIR
DELSY
Дубна
Candle
SESAME
Амман
SRC
Стоутон
APS
Аргон
CHESS
Итака
NSLS
Брукхейвен
SURF
CAM-D
Батон-Руж
CLS
Саскатун
Беркли
ALS
SPEAR
Станфорд
SSRL
LNLS
Кампинас
PLS
Поханг
BSRF
Пекин
SSRF
Шанхай
NSRRC
Тайвань
INDUS
Индора
SSLS
Сингапур
AS
Мельбурн
Photon Factory
NANO-HANA
SuperSOR
VSX
UVSOR
Rits SR
Spring-8

Synchrotron sources in Russia

Siberian Center for Synchrotron Radiation (Budker Institue for Nuclear Physisc, Novosibirsk) in operation since mid 1970-ies
Storage rings VEPP-3 (2 GeV, 120 mA), VEPP-4 (5 GeV, 40 mA) – both **1st generation** (ε ~300 nm·rad)
11 beamlines ssrc.inp.nsk.su

Kurchatov Synchrotron Radiation Source (NRC «Kurchatov Institute», Moscow) in operatiion since early 2000-ies
Siberia-1 (booster, 450 MeV) – 3 VUV beamlines
Siberia-2 – dedicated **2nd generation source** (2.5 GeV, 300 mA, ε ~75 nm·rad), 16 beamlines
www.kcsr.kiae.ru

Zelenograd Synchrotron Radiation Facility (Lukin R&D Institute of Physical Problems), http://www.niifp.ru – under construction

Dubna Electron Synchrotron (JINR) http://wwwinfo.jinr.ru/delsy – project development

International collaboration:
Russian-German beamline at BESSY II http://www.bessy.de/lab_profile/04.rglab/.RGLab
Russian involvement in ESRF consortium (since July 2011)
Russian participation in European XFEL project (scheduled start in 2014, **4th generation source)**

Kurchatov Synchrotron Radiation Centre

X-ray stations	
1	**Protein Crystallography**
2	**Precision X-ray Optics**
3	**X-ray Crystallography and Physical Materials Science**
4	**Medical Imaging**
6	**Energy-Dispersive EXAFS**
7	**Structural Materials Science (SMS)**
8	**X-ray Small Angle Diffraction Cinema (bioobjects)**
9	**Refraction Optics & X-ray Fluorescence Analysis**
10	**X-ray Topography & Microtomography**
VUV stations	
11	**X-ray Photoelectron Spectroscopy**
12	**Optical spectroscopy for Condensed Matter**
13	**Luminescence & Optical Investigations**
Technological stations	
14	**X-ray Standing Waves for Langmuir-Blodgett Films**
15	**Molecular Beam Epitaxy**
16	**LIGA**

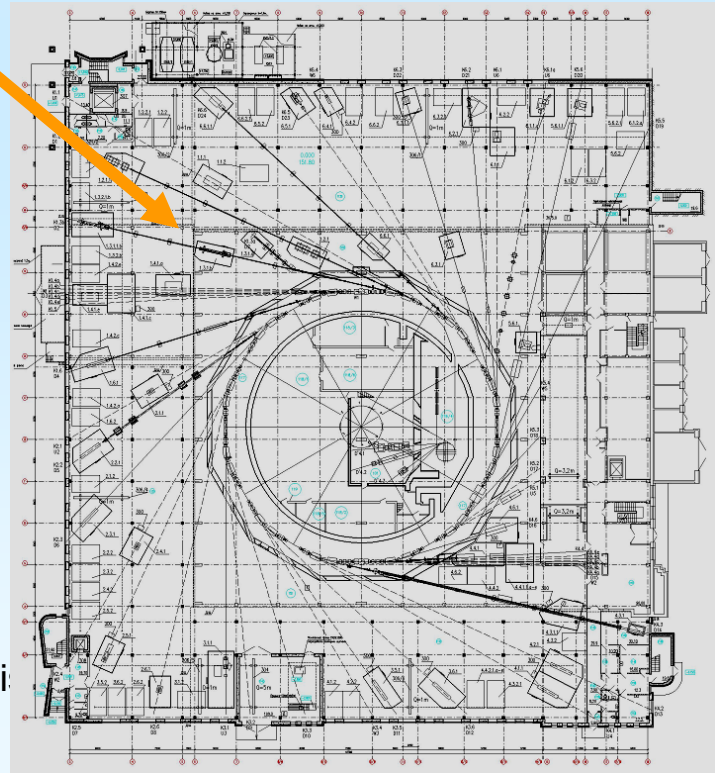

Structural Materials Science beamline

- In the user mode since 2004
- Techniques implemented: XANES/EXAFS, XRD, SAXS
- Mission: combined multitechnique X-ray diagnostics of non-crystalline and nanostructured functional materials
- Objects: supported catalysts, metal/polymer hybrids, metal glasses and alloys, transition metal cluster and coordination compounds, colloidal suspensions

SMS : optical scheme

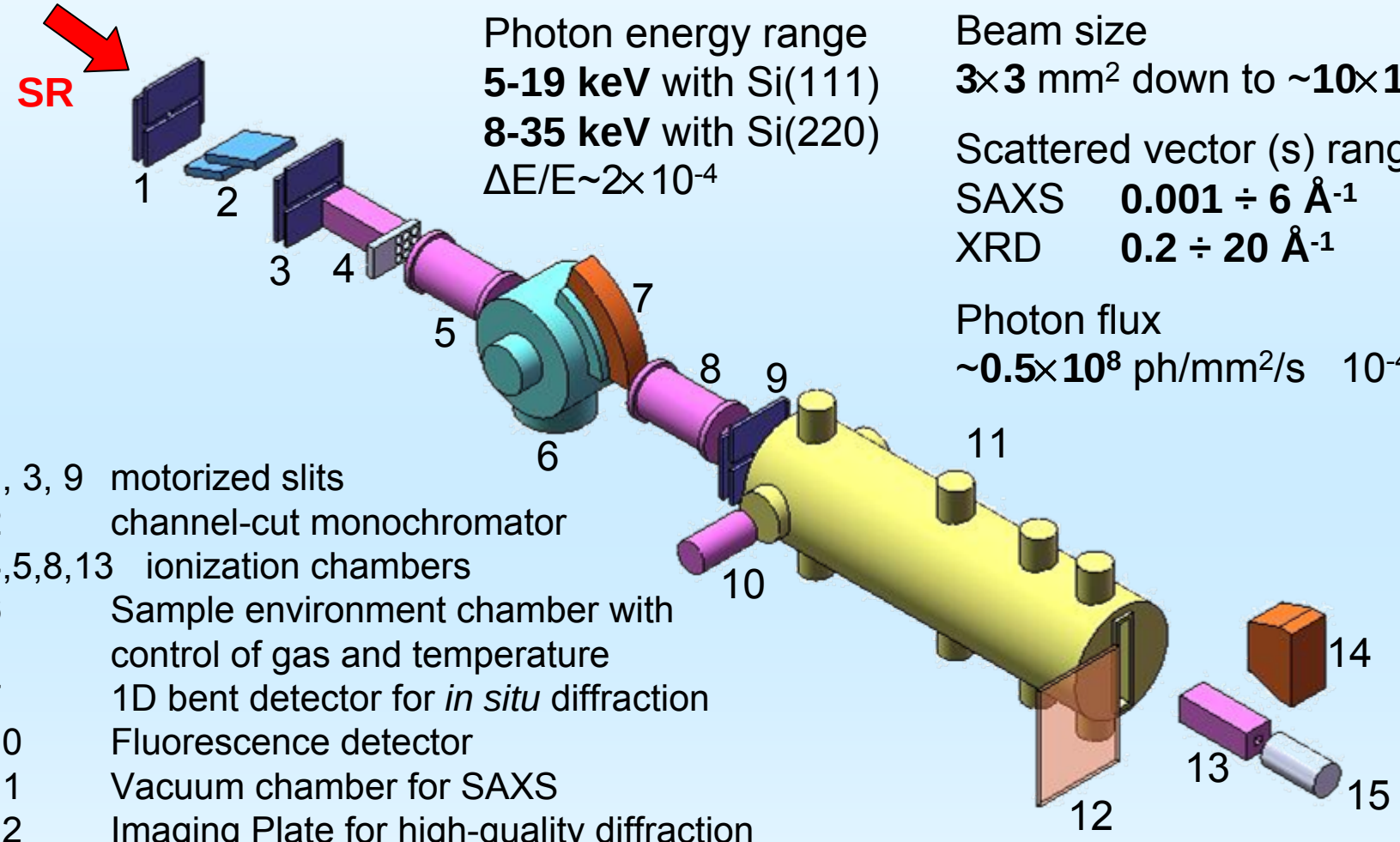

Photon energy range
5-19 keV with Si(111)
8-35 keV with Si(220)
$\Delta E/E \sim 2 \times 10^{-4}$

Beam size
3×3 mm^2 down to **~10×10** mkm^2

Scattered vector (s) range
SAXS **0.001 ÷ 6 Å^{-1}**
XRD **0.2 ÷ 20 Å^{-1}**

Photon flux
~0.5×10^8 ph/mm^2/s 10^{-4} $\Delta\lambda/\lambda$

1, 3, 9	motorized slits
2	channel-cut monochromator
4,5,8,13	ionization chambers
6	Sample environment chamber with control of gas and temperature
7	1D bent detector for *in situ* diffraction
10	Fluorescence detector
11	Vacuum chamber for SAXS
12	Imaging Plate for high-quality diffraction
14	1D position sensitive detector for SAXS
15	Transmitted beam position monitor

Modes of measurements

in situ time-resolved diffraction

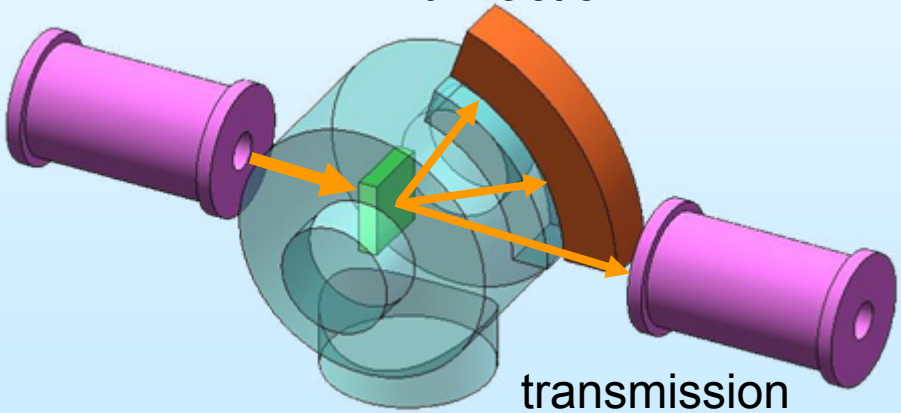

transmission XAFS

SAXS

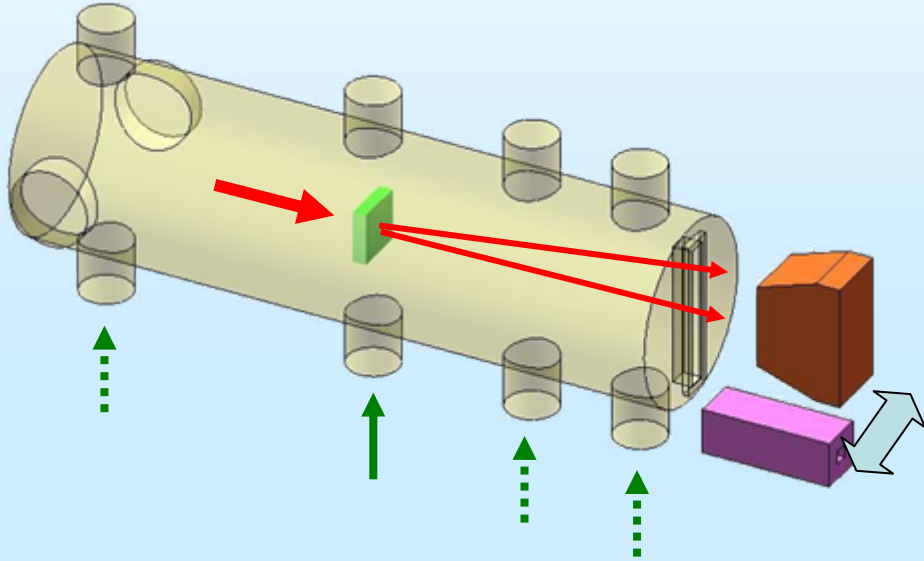

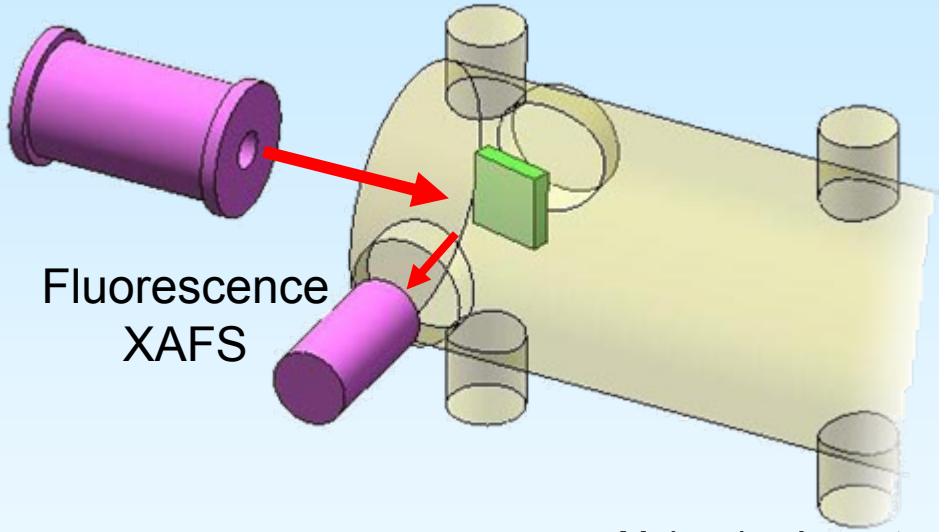

Fluorescence XAFS

Structural diffraction

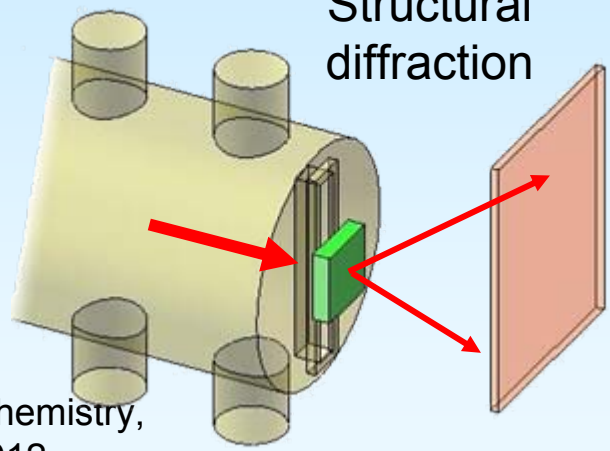

Most demanded measurements: transmission XAFS with an autosampler

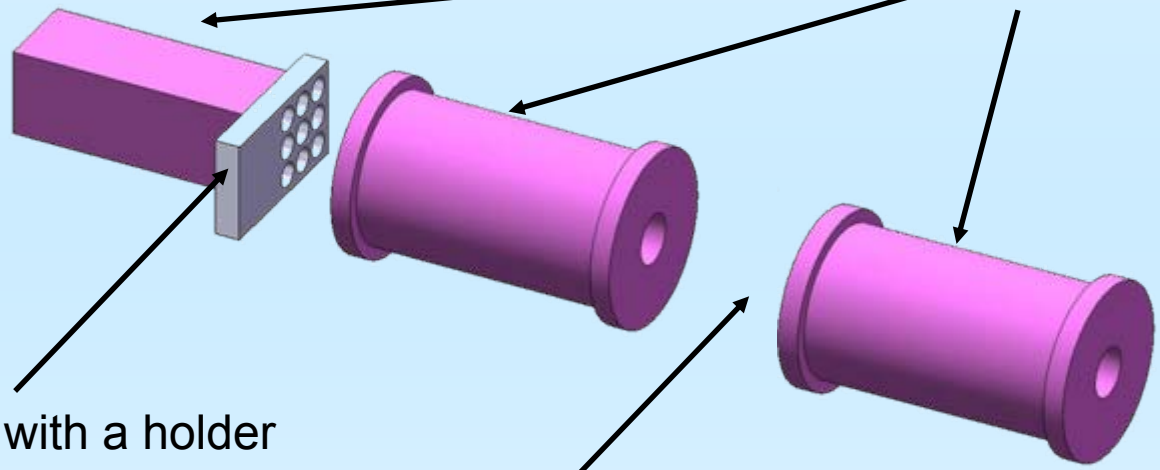

Autosampler with a holder for 9 samples

Reference sample for the energy scale calibration (metal foil)

Sample temperature control

Limited capabilities for temperature variation:

-120°C or
-196°C

Chromel-alumel (Type K) thermocouple

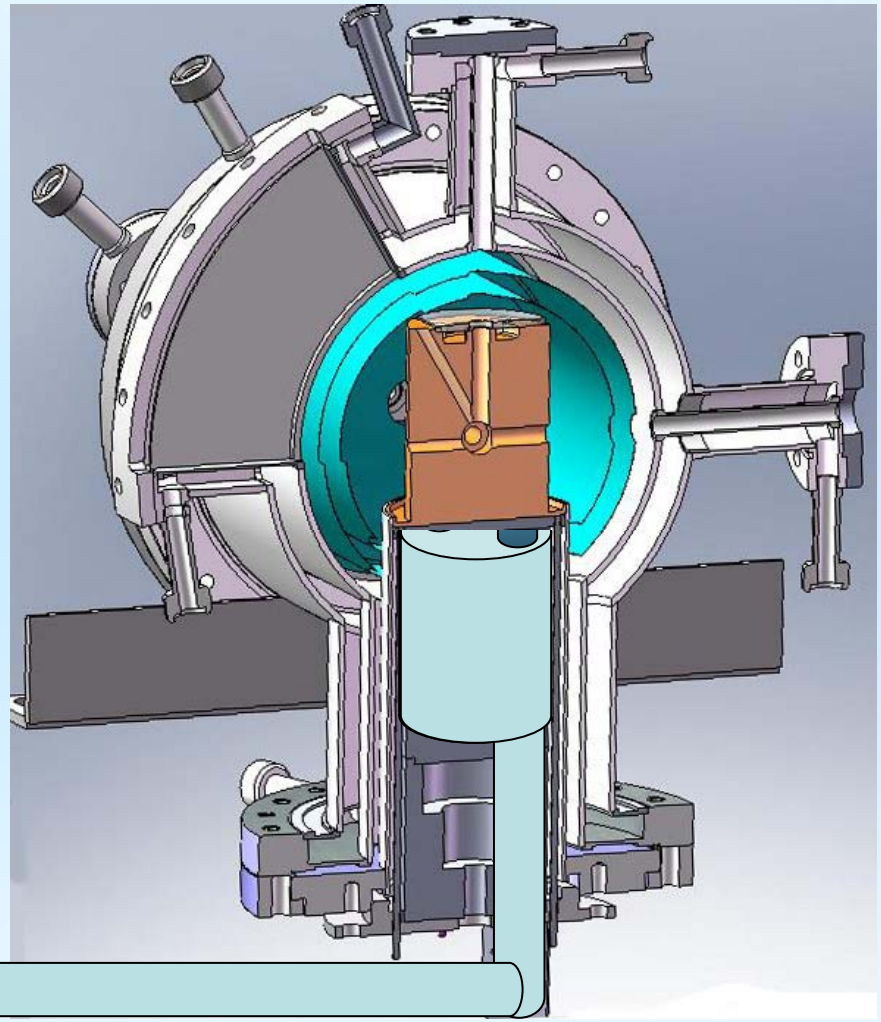

20-550°C

Thermostabilization
±1°C

Cooling
From 500°C down to -120°C ~ 1 hour

N_2, cold gas or liquid

4 × 350 W

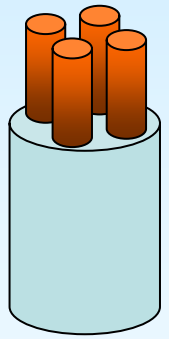

Closed-cycle He-refrigerator

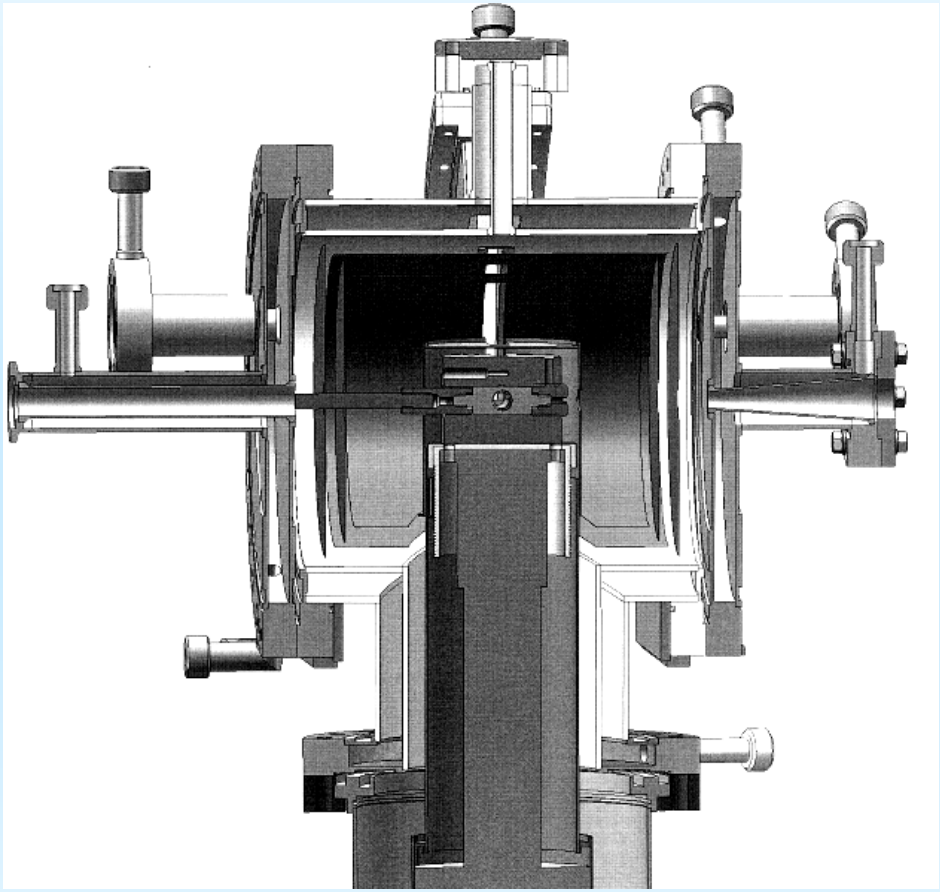

The minimum temperature reached 5.5K + precise temperature variation up to room temperature

Gas inlet system

- Three-component mixtures
- Inert gases: **He, N_2, Ar**
- Redox processing: **O_2, H_2**
- Catalytic substrates: **CO, CH_4**

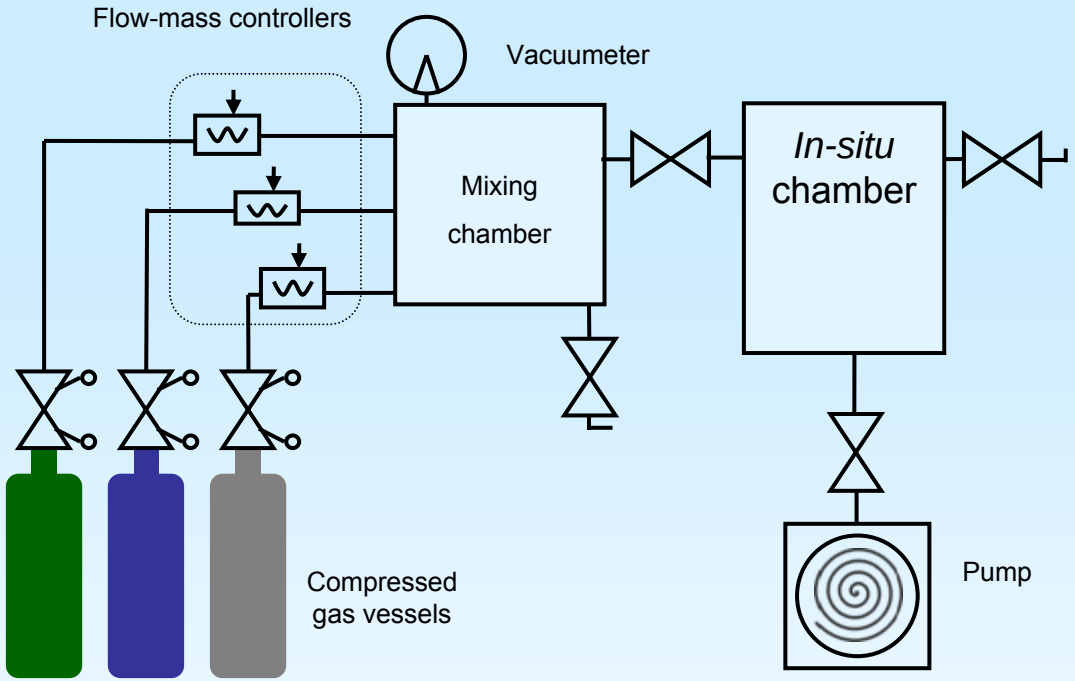

Combined use of XAFS, XRD and SAXS

- **XANES** - oxidation state of heavy atoms + coordination symmetry
- **EXAFS** - local neighborhood of a given heavy atom
- **XRD** - long-range order, phase composition, size of crystallites
- **SAXS** - size and shape of nanoparticles or pores in a range of 1-100 nm

X-ray absorption spectroscopy: basics

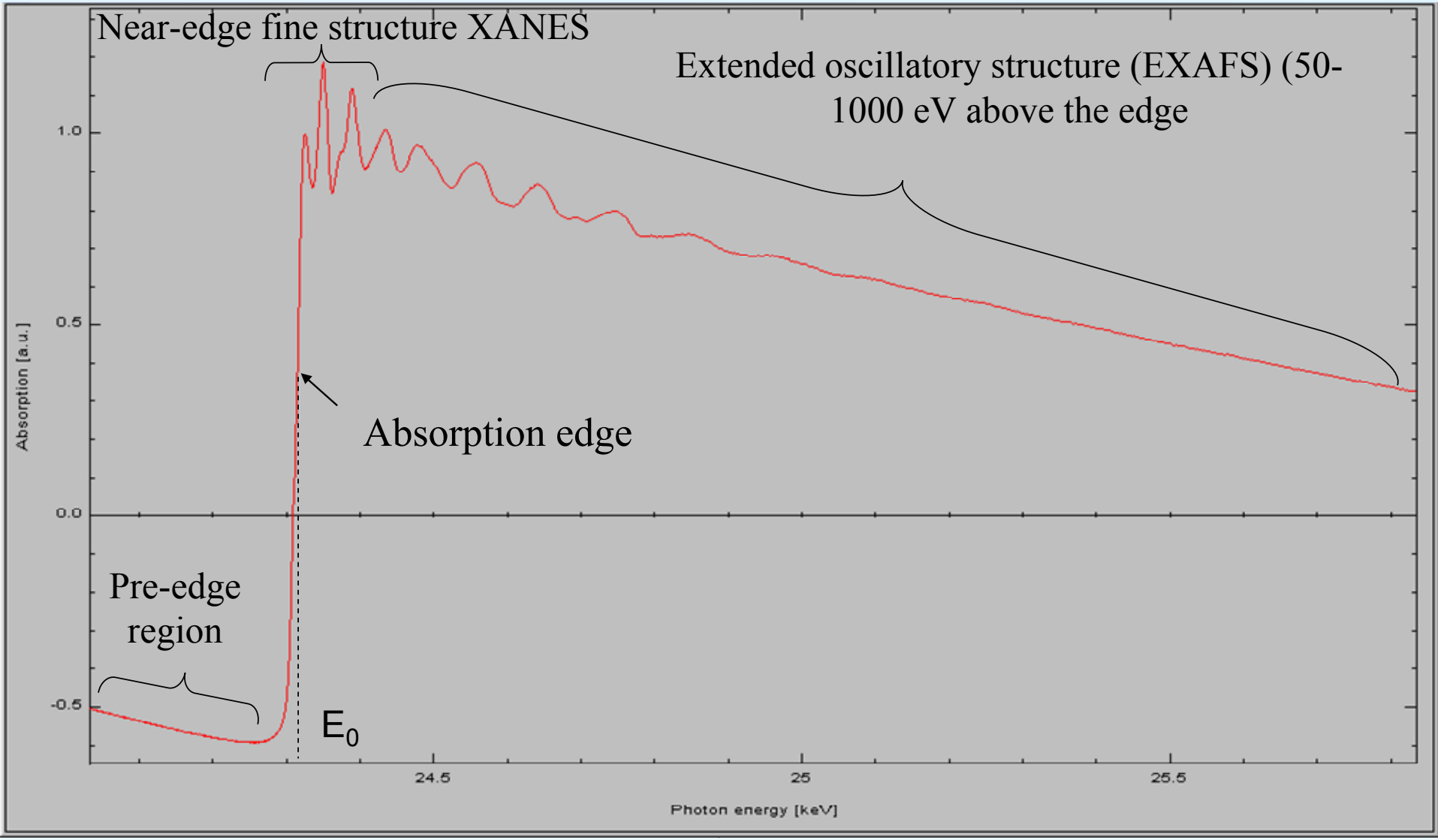

XANES: origin

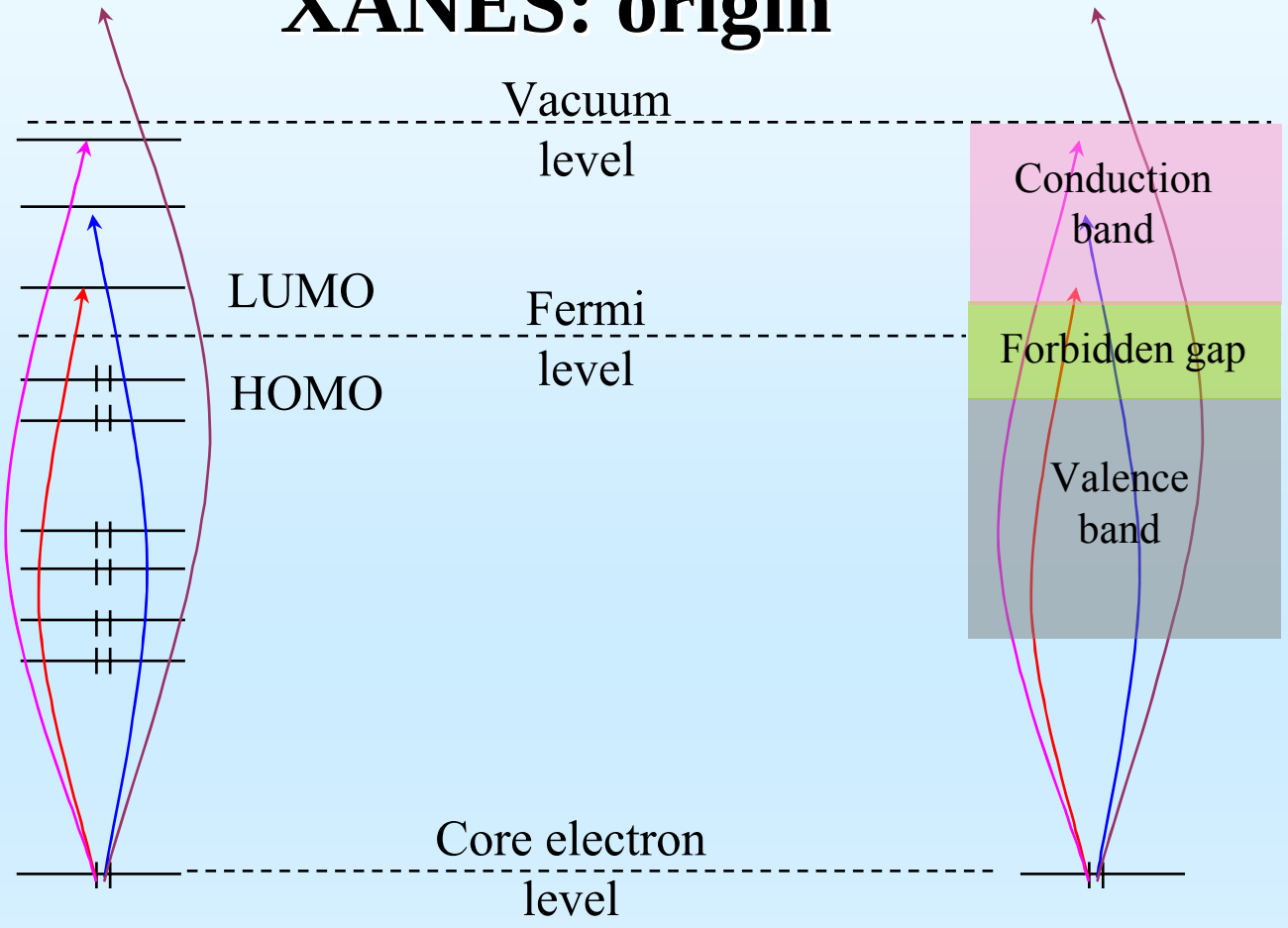

XANES probes the energy distribution of certain symmetry-allowed MOs or DOS features above the Fermi level

Fermi's golden rule:

$\mu \sim |\langle f | V | i \rangle|^2$, f,i – wave functions of the final and initial states, V – dipole moment operator

EXAFS: origin

Initial state: electron on the core level

Final state: outgoing photoelectron wave

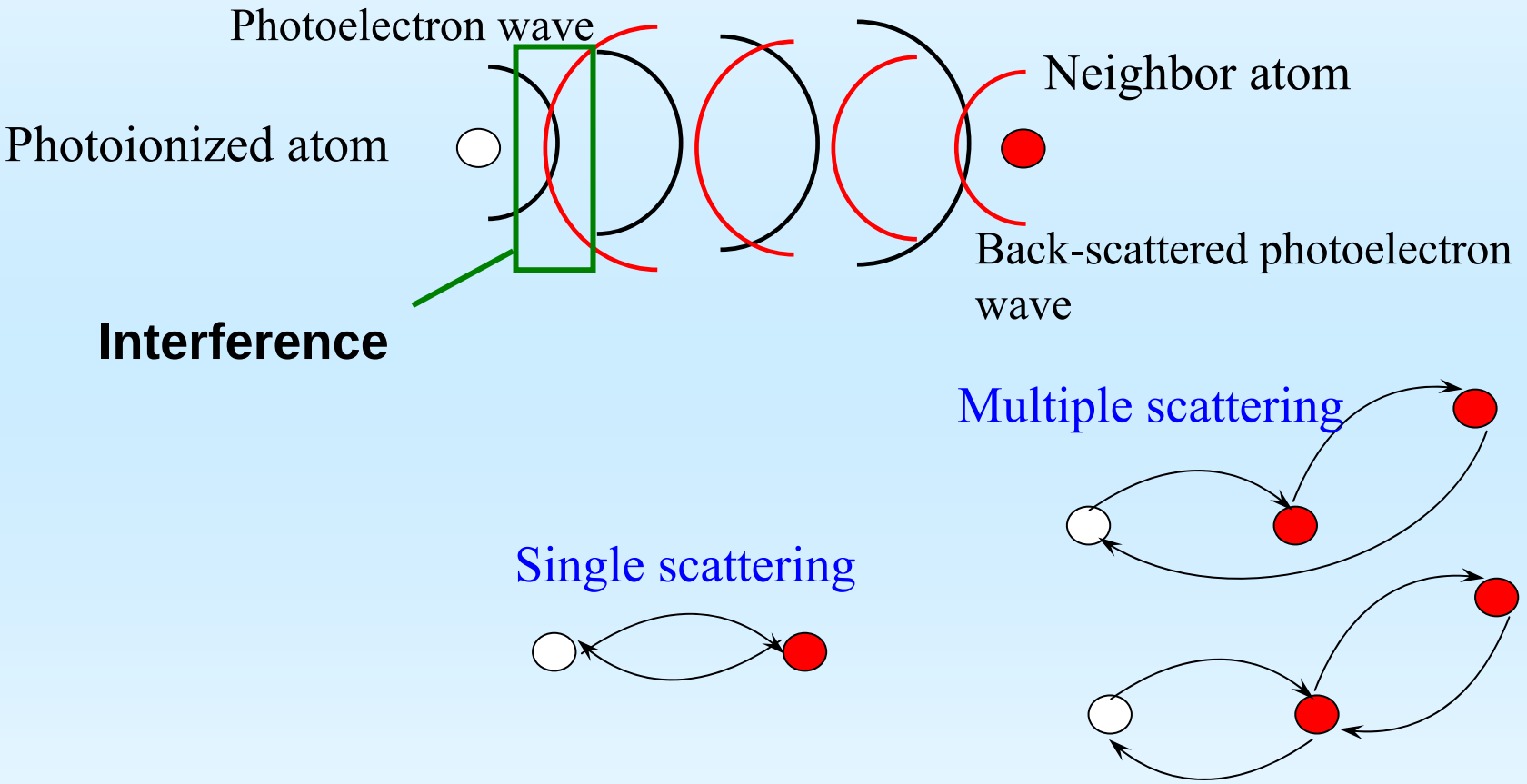

Local-structrure parameters of the central atom can be retrieved from EXAFS

$$\chi(k) = \sum_j \frac{S(k) N_j}{k r_j^2} \left| f_j(k,\pi) \right| \sin(2kr_j + \varphi_j(k)) e^{-2\sigma_j^2 k^2} e^{-2r_j/\lambda(k)}$$

χ - normalized background-subtracted EXAFS-signal
k – photoelectron vector modulus ($\equiv 2\pi/\lambda$)
S – Extrinsic loss coefficient (0.7-1.0)
N – coordination number in the j-th coordination sphere
r – interatomic distance
f – backscattering amplitude
φ – phase shift
σ– Debye-Waller factors
λ– photoelectron mean-free path

Techniques development

- Complementary utilization of XAFS, SAXS and XRD in structural diagnostics of complex poorly ordered materials
- Structural diagnostics of functional materials *in situ* under operational conditions
- Online structural monitoring of dynamical processes (phase transitions, chemical reactions)
- Local-sensitive microbeam techniques applied to microheterogeneous specimens

Experiments aimed at techniques development

- **Time-resolved diffraction**
- **Spatially resolved diffraction**
- **XAFS monitoring of chemical reactions in aqueous solutions**

Pd acetate reduction with molecular hydrogen

Evolution of the diffraction pattern exposure 1 min)

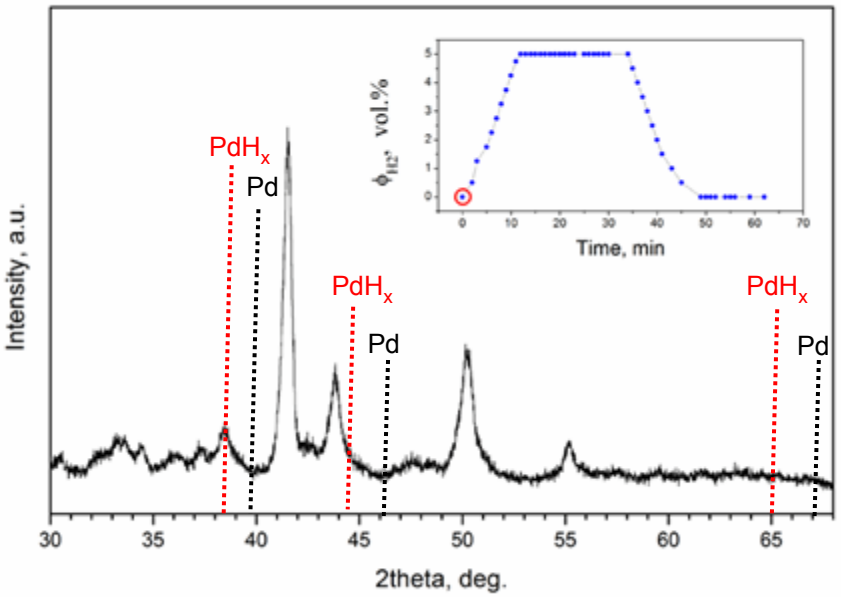

Pd K-edge XANES

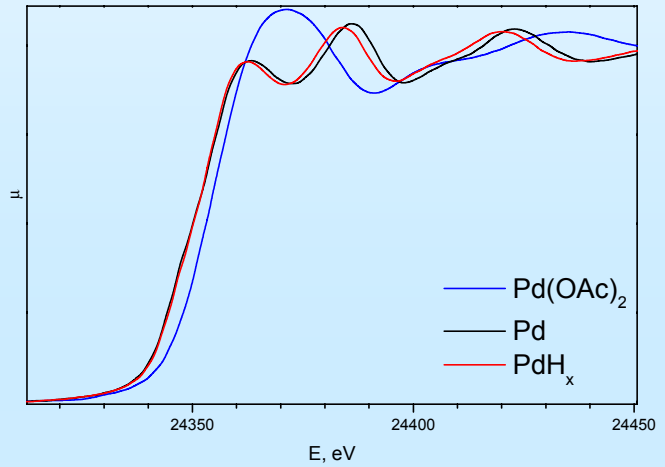

Pd K-edge EXAFS

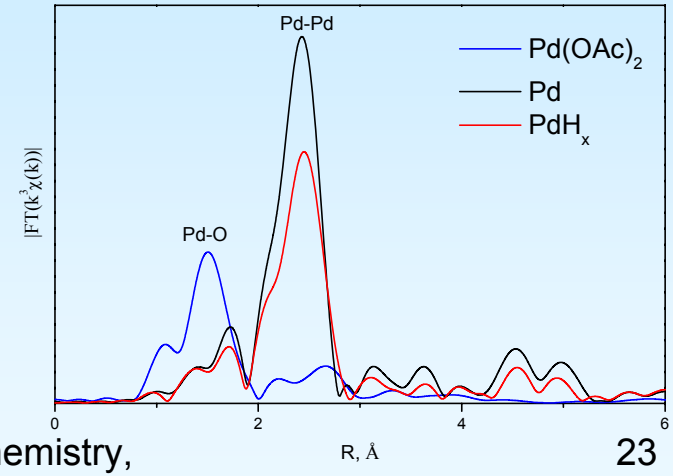

Morphology of LTSC Nb_3Sn-wires

(in a collaboration with Prof. E.A. Dergunova, et al., VNIINM)

A perpendicular cut

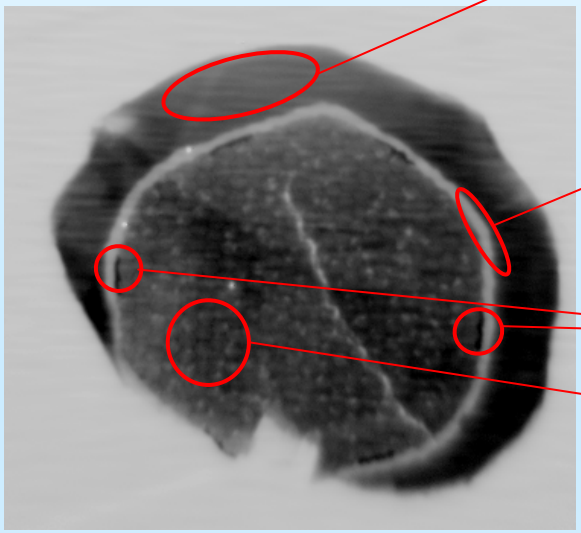

A parallel cut

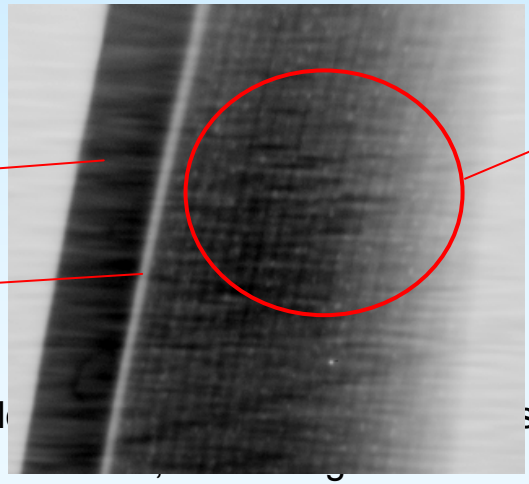

X-ray Tomographic reconstruction (R.A. Senin, A.S. Khlebnikov)

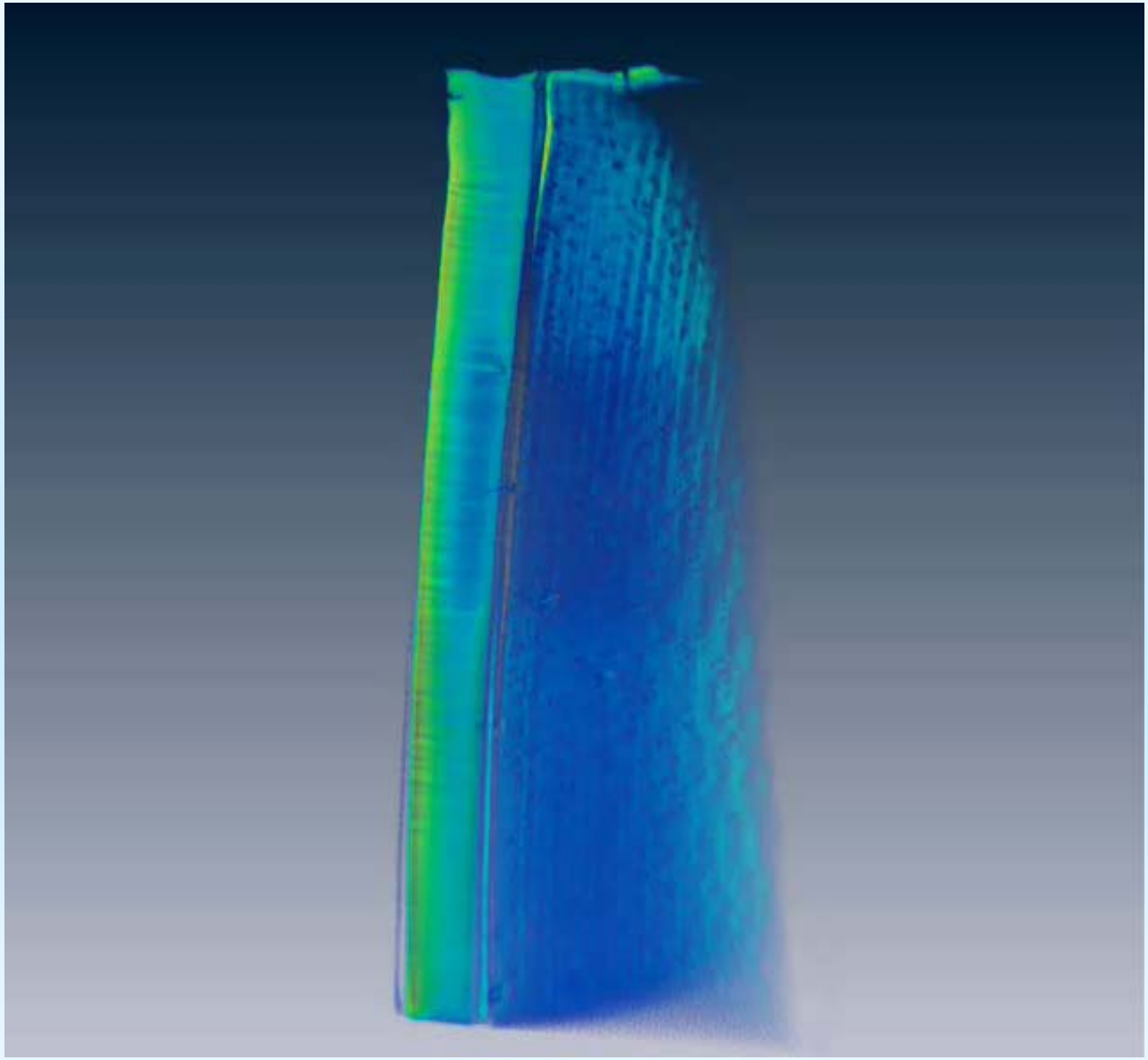

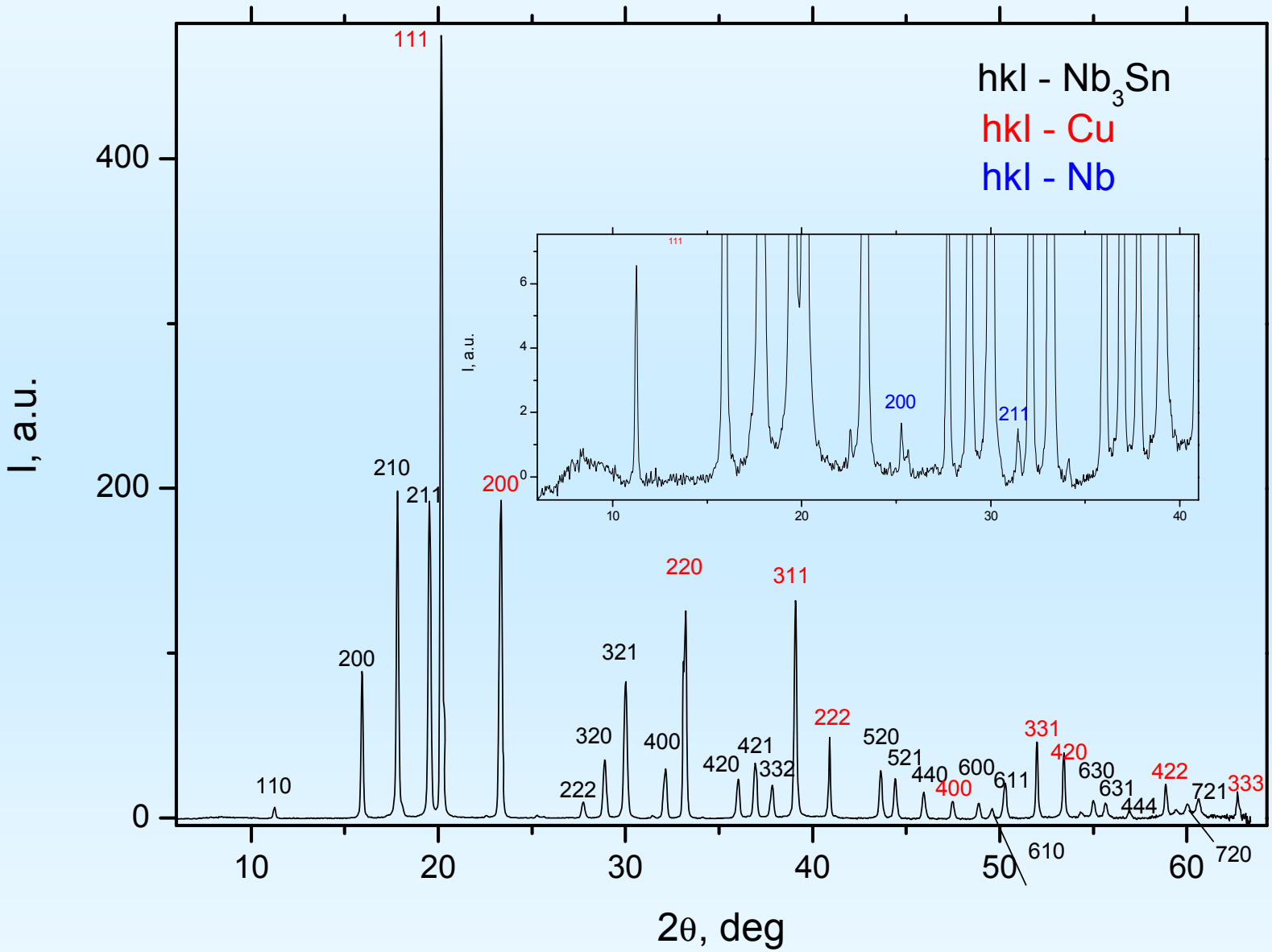
hkl - Nb3Sn
hkl - Cu
hkl - Nb
I, a.u.
2θ, deg
111
210
211
200
110
200
321
320
222
400
220
420
421
332
311
222
520
521
440
400
600
611
331
420
630
631
444
422
721
333
610
720
I, a.u.
111
200
211

X-ray diffraction mapping of the heterogeneous sample (beamsize ~150 μm)

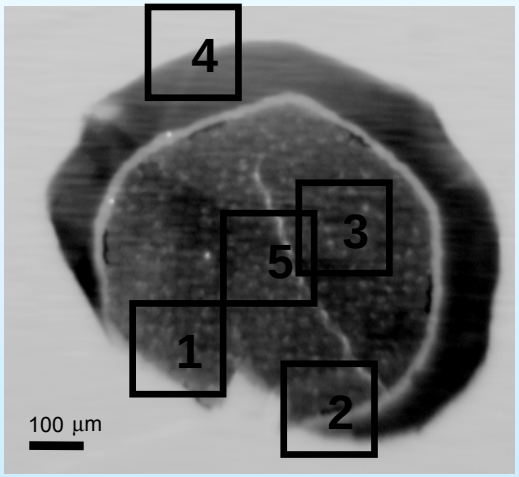

Spot 2

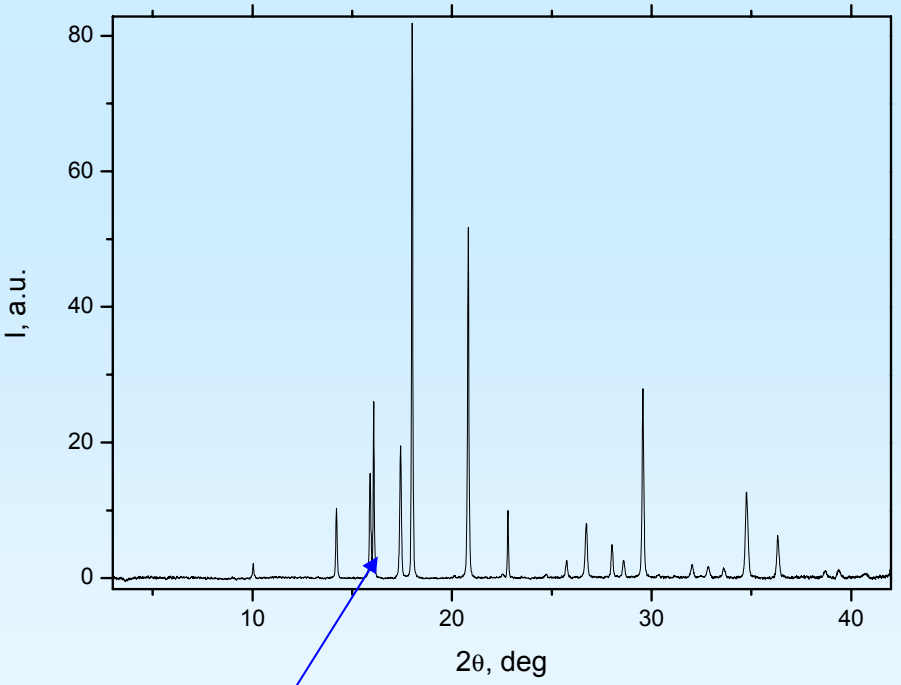

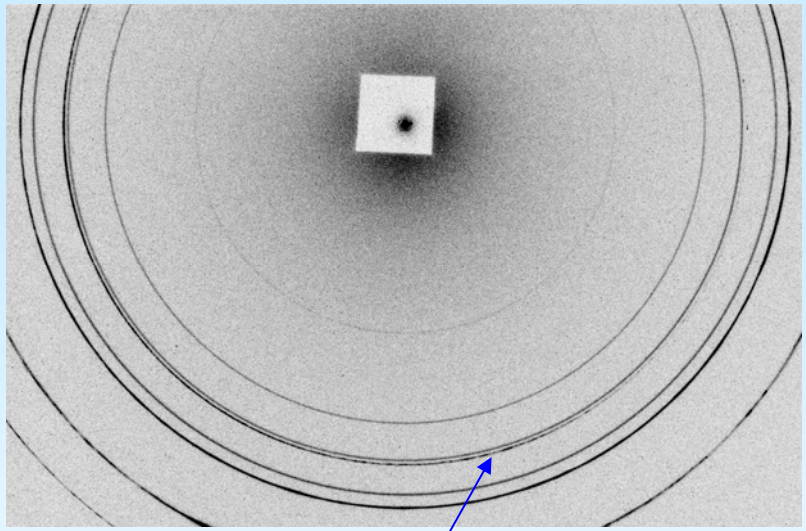

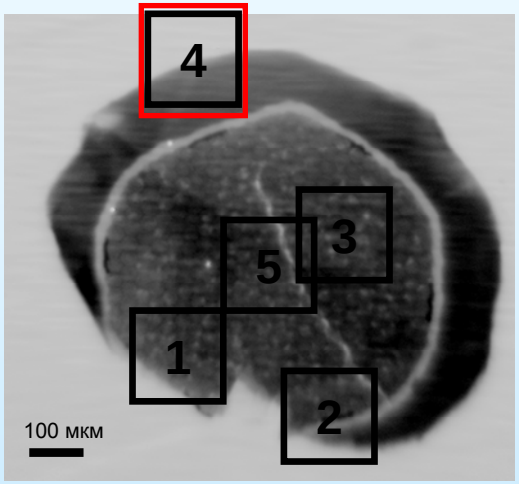

Spot 4

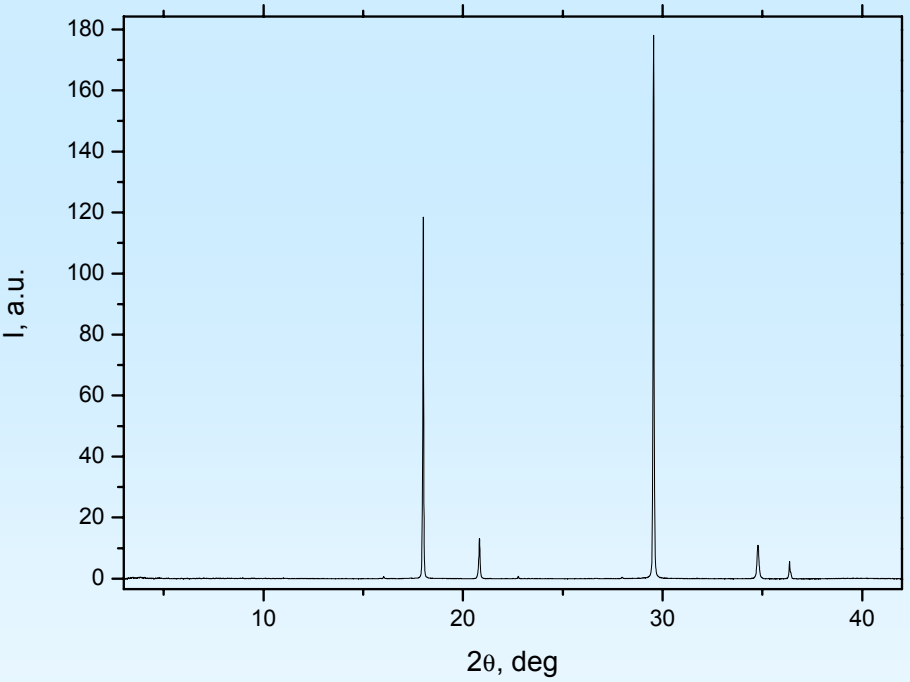

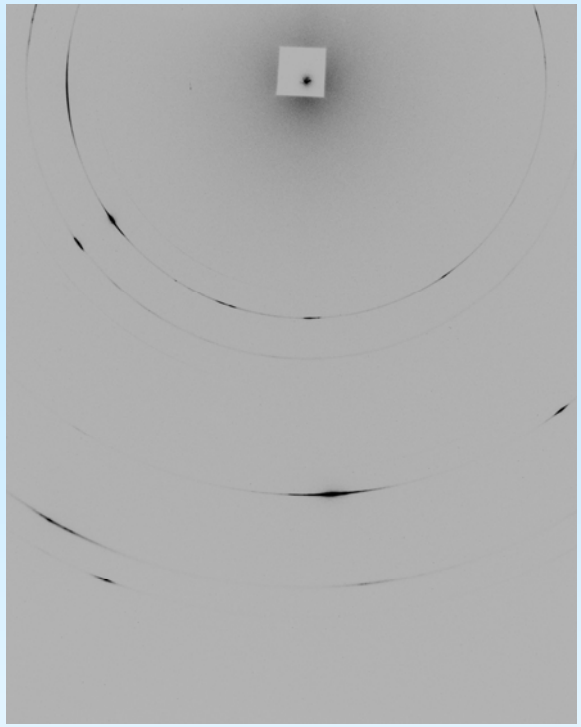

Only strongly textured Cu

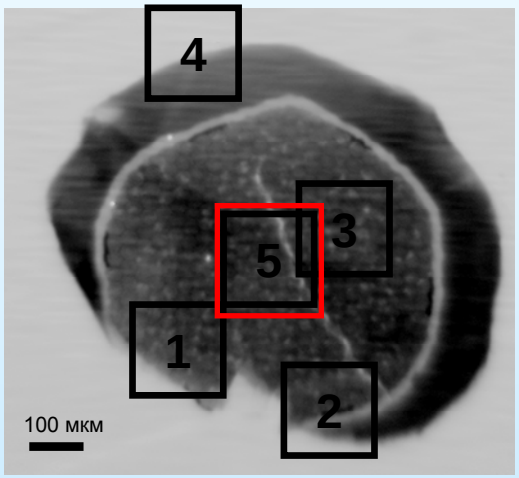

Spot 5

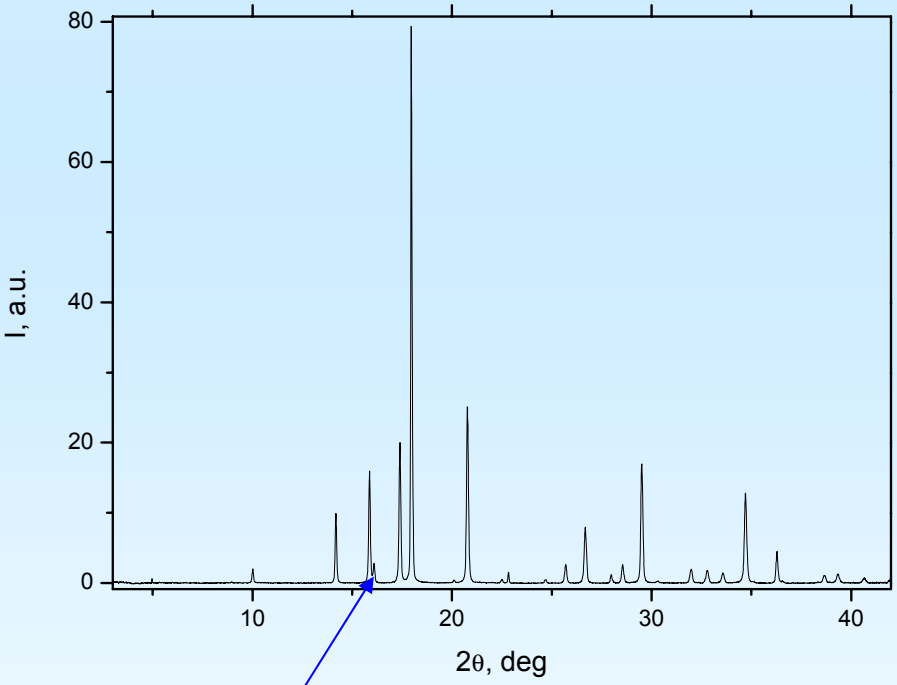

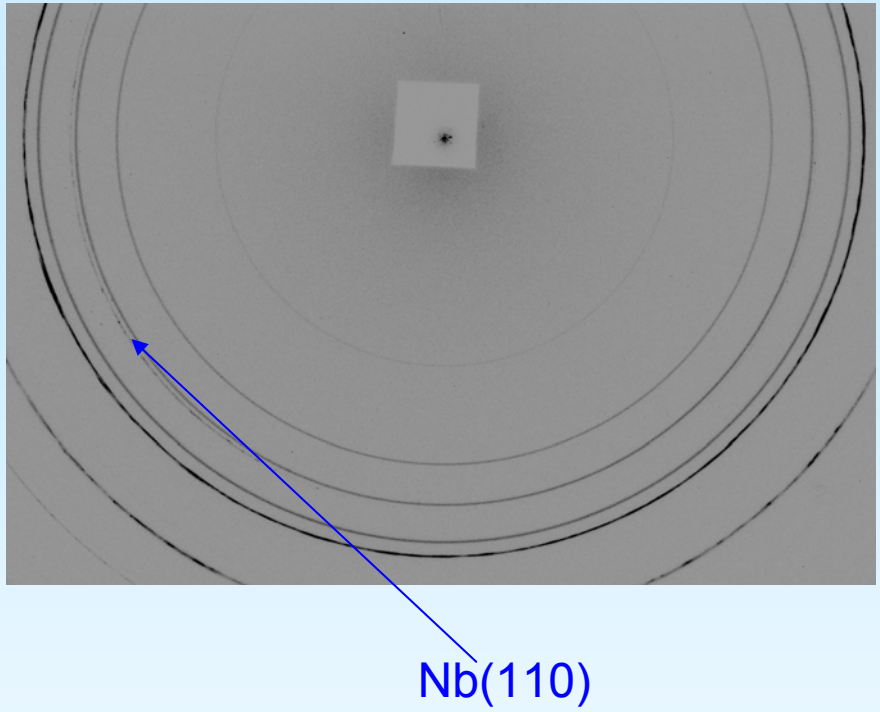

The use of anomalous diffraction to emphasized the contribution of Nb-phases

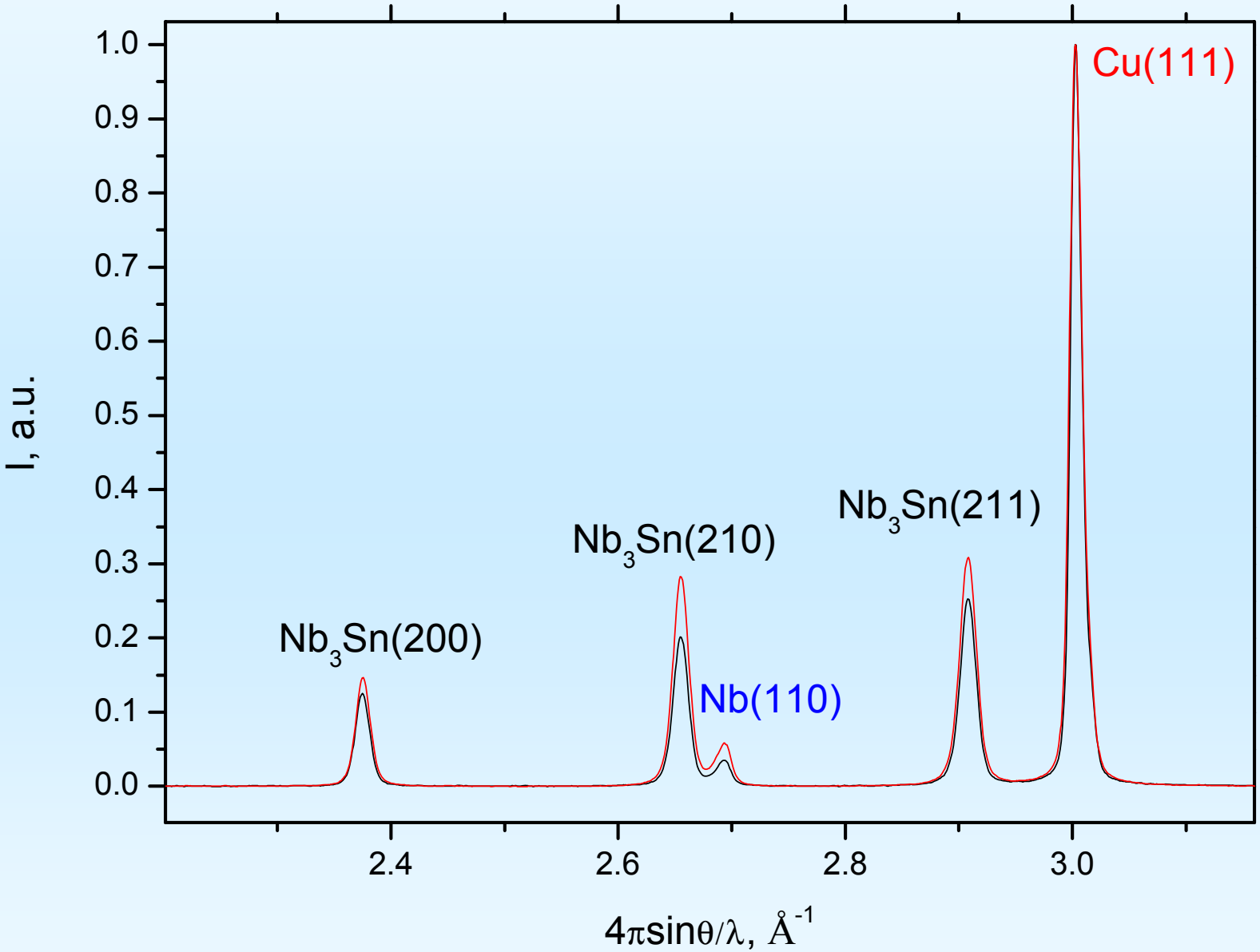

Low-temperature diffraction study

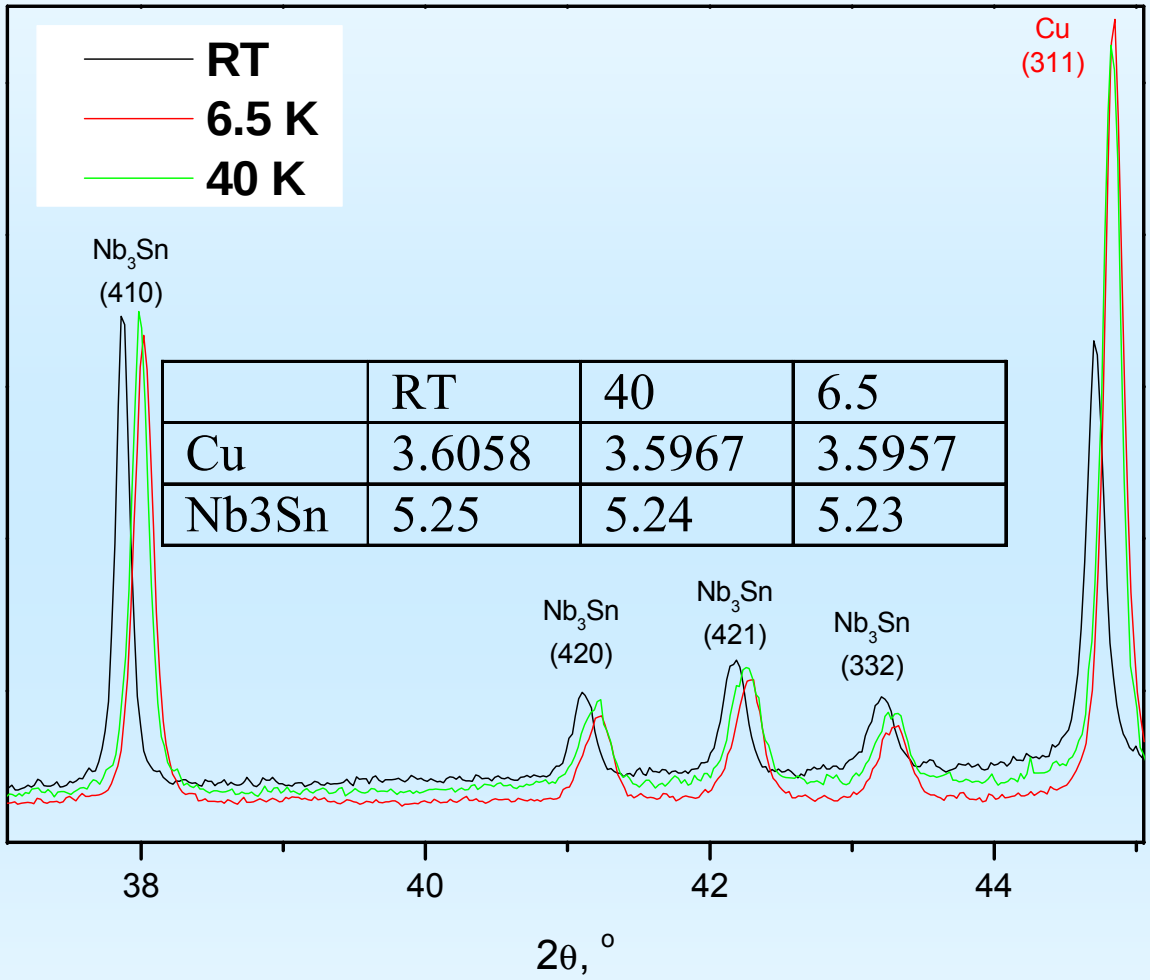

I, a.u.

	RT	40	6.5
Cu	3.6058	3.5967	3.5957
Nb3Sn	5.25	5.24	5.23

No structural phase transition cubic →tetragonal

APPLIED PHYSICS LETTERS **99**, 122507 (2011)

Evidence that the upper critical field of Nb_3Sn is independent of whether it is cubic or tetragonal

Jian Zhou, Younjung Jo,[a)] Zu Hawn Sung, Haidong Zhou, Peter J. Lee, and David C. Larbalestier[b)]

Redox chemistry of Br-containing aqueous solutions from Br K-edge XANES

$NaBrO_3$ (solid)

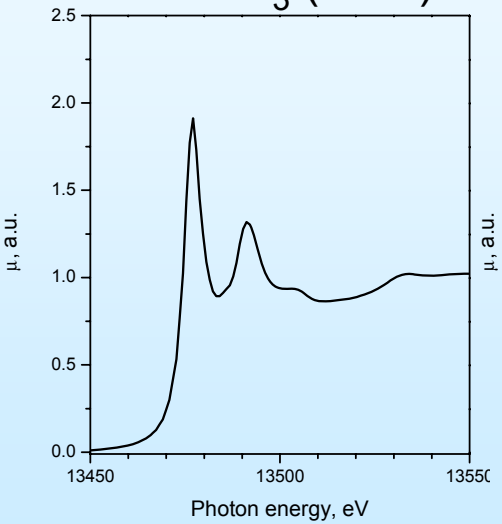

$NaBrO_3$ (aq.)

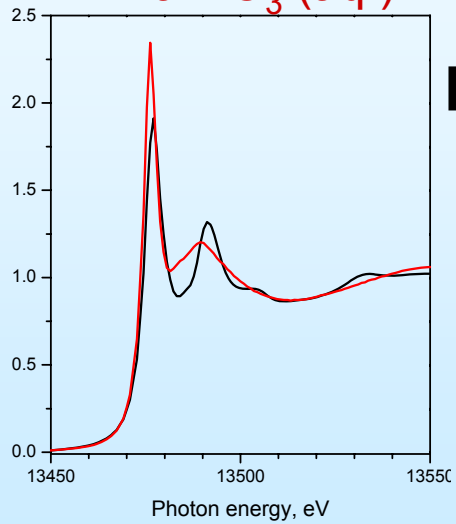

$BrO_3^- + 5Br^- + 6H^+ \rightarrow 3Br2 + 3H_2O$

KBr (solid)

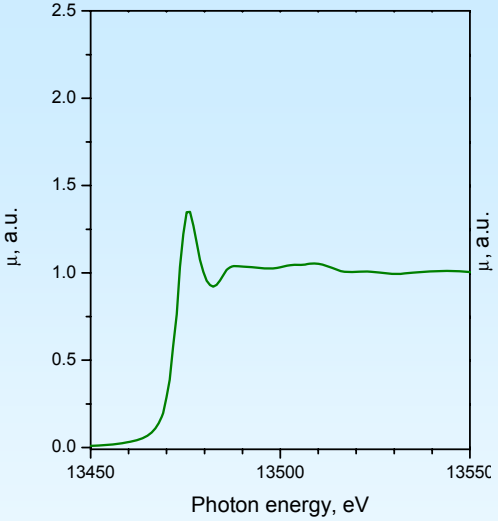

KBr (aq.)

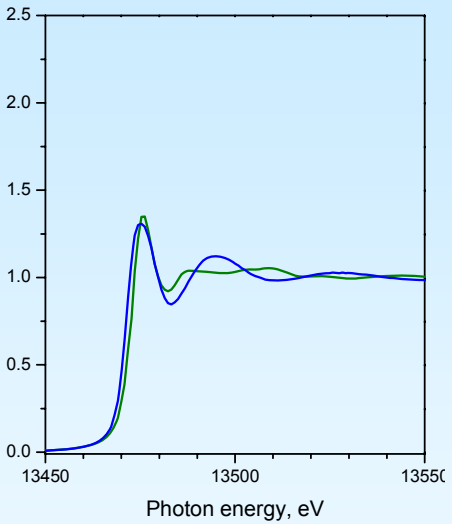

$1NaBrO_3$:5KBr (aq.)

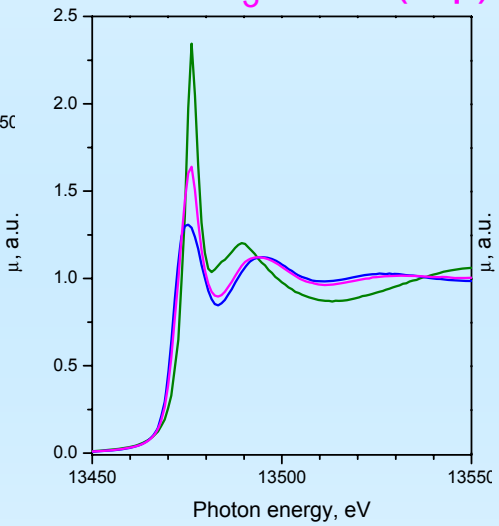

$+H^+$ (Br_2)

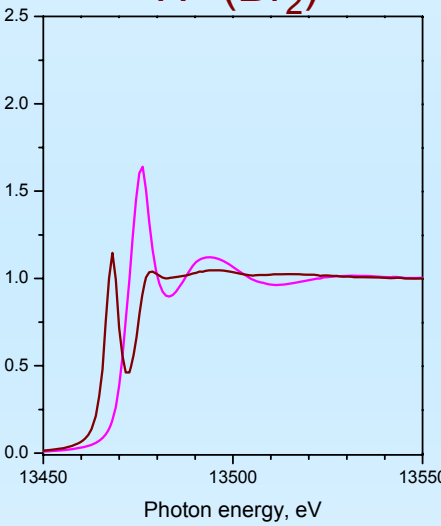

Composition of the mixture: linear combination fit

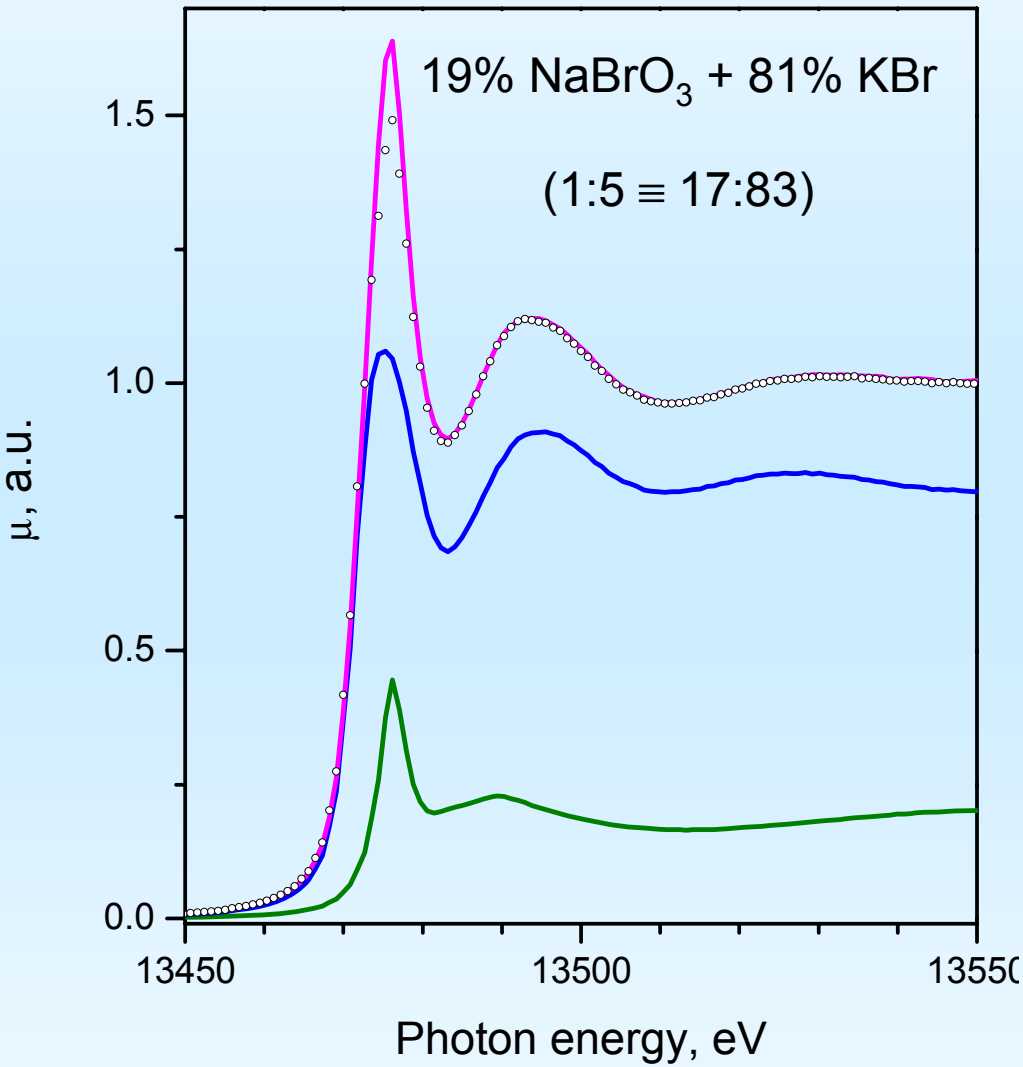

Examples of combined studies of complex materials

- **Pd/Cu catalysts for the mild CO oxidation**
- **Water-soluble Al activated with $Ga_{85}In_{15}$ eutectic alloy**

$(Pd,Cu)Cl_x/\gamma\text{-}Al_2O_3$ catalysts for the mild CO oxidation

(in a collaboration with L.G. Bruk)

Series of samples studied

- Starting reagents $CuCl_2 \cdot 2H_2O$ and $PdCl_2$
- Impregnation solutions $CuCl_2$ and $CuCl_2$-$PdCl_2$
- Pure support γ-Al_2O_3
- Model systems $CuCl_2/\gamma$-Al_2O_3 , $PdCl_2$,KCl /γ-Al_2O_3
- Actual catalyst $PdCl_2$,$CuCl_2/\gamma$-Al_2O_3 “as is”
- Catalyst $PdCl_2$,$CuCl_2/\gamma$-Al_2O_3 under action of CO (only CO, $CO+H_2O$, $CO+H_2O+O_2$)

Problems addressed by the structural study

- The chemical nature of active sites
- The mechanism explaining the synergism in the Cu and Pd catalytic activity

The genesis of active sites: XRD

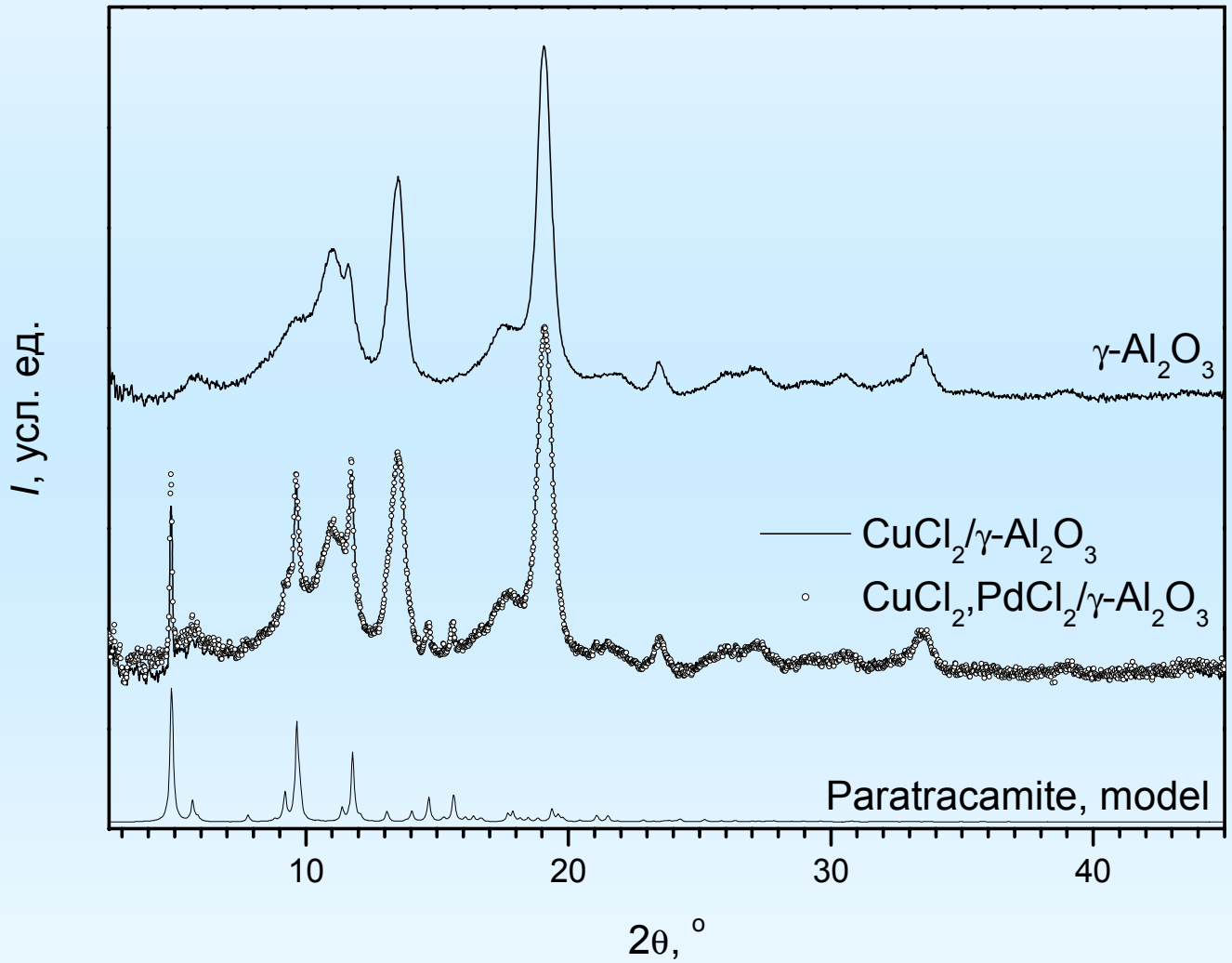

Cu^{2+} is adsorbed on γ-Al_2O_3 from $CuCl_2$ aqueous solutions as polycrystalline paratacamite $Cu_2Cl(OH)_3$

Palladium is "diffraction-silent"

The genesis of active sites: Cu K-edge EXAFS

Sample	Coord. sphere	N	R, Å	σ^2, Å^2	ΔE, eV	R_f
$CuCl_2 \cdot 2H_2O$	Cu-O	2	1.95 (1.94)*	0.0045	2.5	0.030
	Cu-Cl	2	2.27 (2.28)	0.0035		
	Cu…Cl	2	2.86 (2.93)	0.0148		
Solution 1 ($CuCl_2$)	$Cu\text{-}O_{eq}$	4	1.97	0.0043	0.6	0.021
	$Cu\text{-}O_{ax}$	2	2.29	0.0210		
Solution 2 ($CuCl_2$, $PdCl_2$)	$Cu\text{-}O_{eq}$	4	1.97	0.0044	0.7	0.018
	$Cu\text{-}O_{ax}$	2	2.30	0.0203		
$Cu/\gamma\text{-}Al_2O_3$	$Cu\text{-}O_1$	2	1.99 (1.98)	0.0026	0.4	0.016
	$Cu\text{-}O_2$	3	2.05 (2.11)	0.0266		
	Cu...Cl	1	2.85 (2.79)	0.0065		
	$Cu...Cu_1$	4	3.09 (3.06)	0.0186		
	$Cu...Cu_2$	2	3.47 (3.41)	0.0093		
$Cu,Pd/\gamma\text{-}Al_2O_3$	$Cu\text{-}O_1$	2	1.99 (1.98)	0.0028	1.2	0.016
	$Cu\text{-}O_2$	3	2.09 (2.11)	0.0400		
	Cu...Cl	1	2.89 (2.79)	0.0072		
	$Cu...Cu_1$	4	3.09 (3.06)	0.0157		
	$Cu...Cu_2$	2	3.47 (3.41)	0.0116		

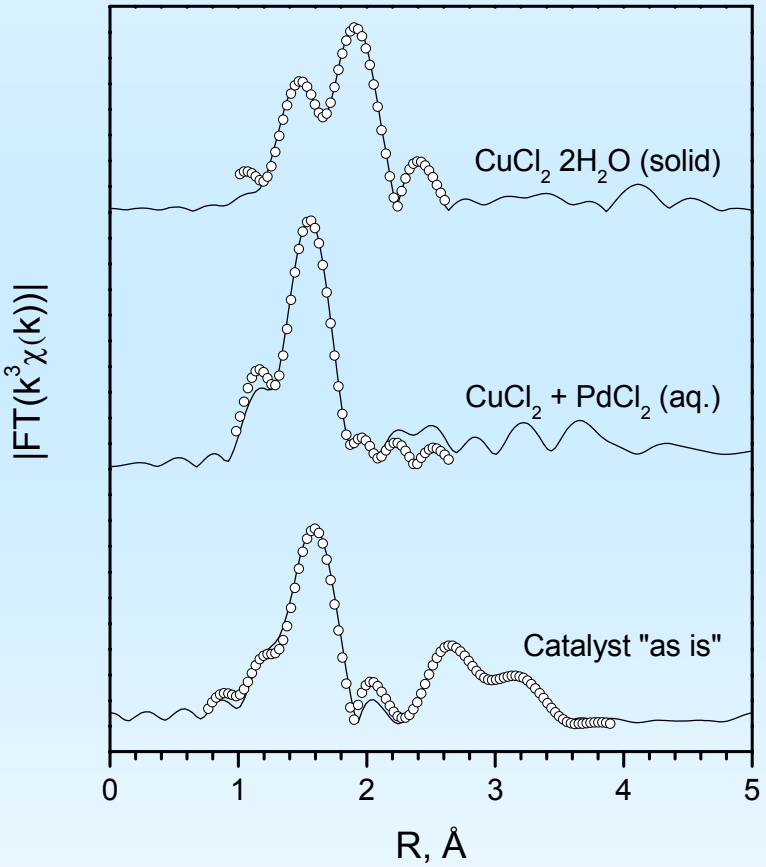

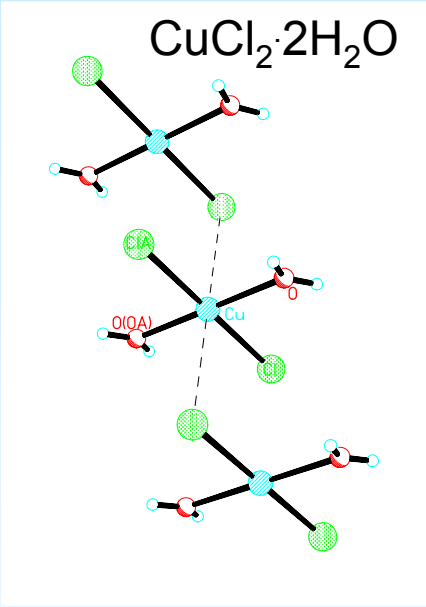

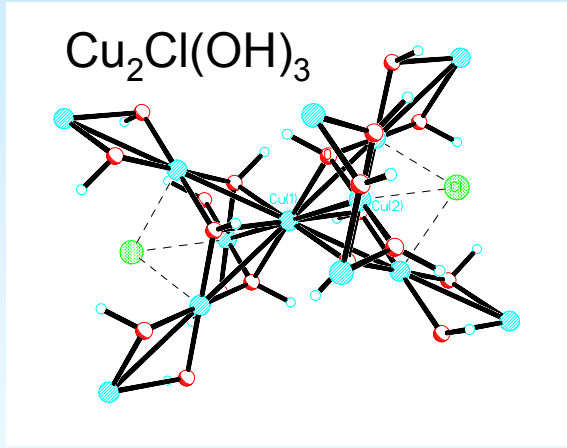

The genesis of active sites: Pd K-edge EXAFS

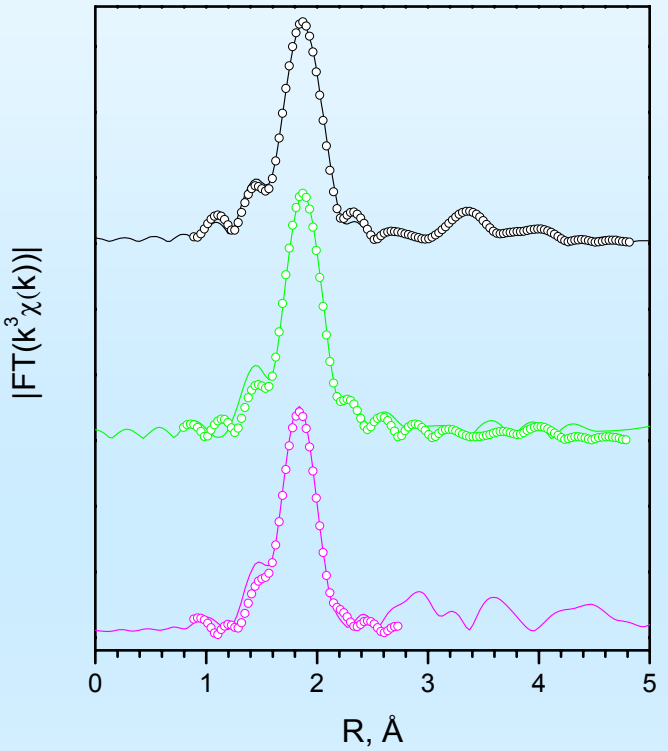

Sample	Coord. sphere	N	R, Å	σ^2, Å^2	ΔE, eV	R_f
$PdCl_2$	Pd-Cl	4	2.29 (2.30-2.31)*	0.0027	4.5	0.007
	Pd...Pd	4	3.28 (3.28-3.33)	0.0146		
	Pd…Cl	1	3.37 (3.34)	0.0013		
	Pd...Pd_2	1	3.72 (3.77)	0.0040		
	Pd-Cl-Pd-Cl	2	4.57 (4.60-4.62)	0.0026		
Solution 2 ($CuCl_2$, $PdCl_2$)	Pd-Cl	4	2.28	0.0022	4.85	0.030
	Pd-Cl-Pd-Cl	2	4.56	0.0050		
Cu,Pd/γ-Al_2O_3	Pd-Cl_1	3	2.26	0.0015	2.9	0.019
	Pd-Cl_2	1	2.36	0.0015		

Pd is adsorbed on γ-Al_2O_3 from aqueous solutions of $PdCl_2$ as isolated square-planar $[PdCl_4]^{2-}$ anions
No specific interactions Cu…Pd are observed

β-$PdCl_2$ (Pd_6Cl_{12})

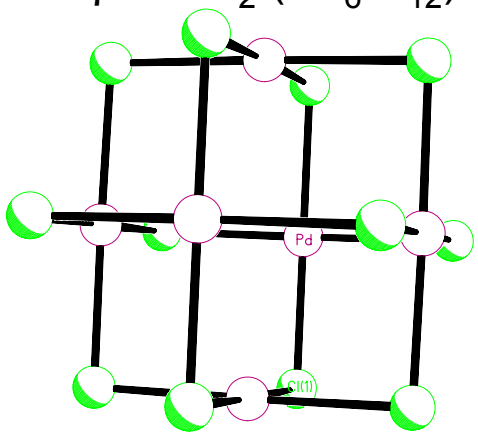

Low-temperature EXAFS study

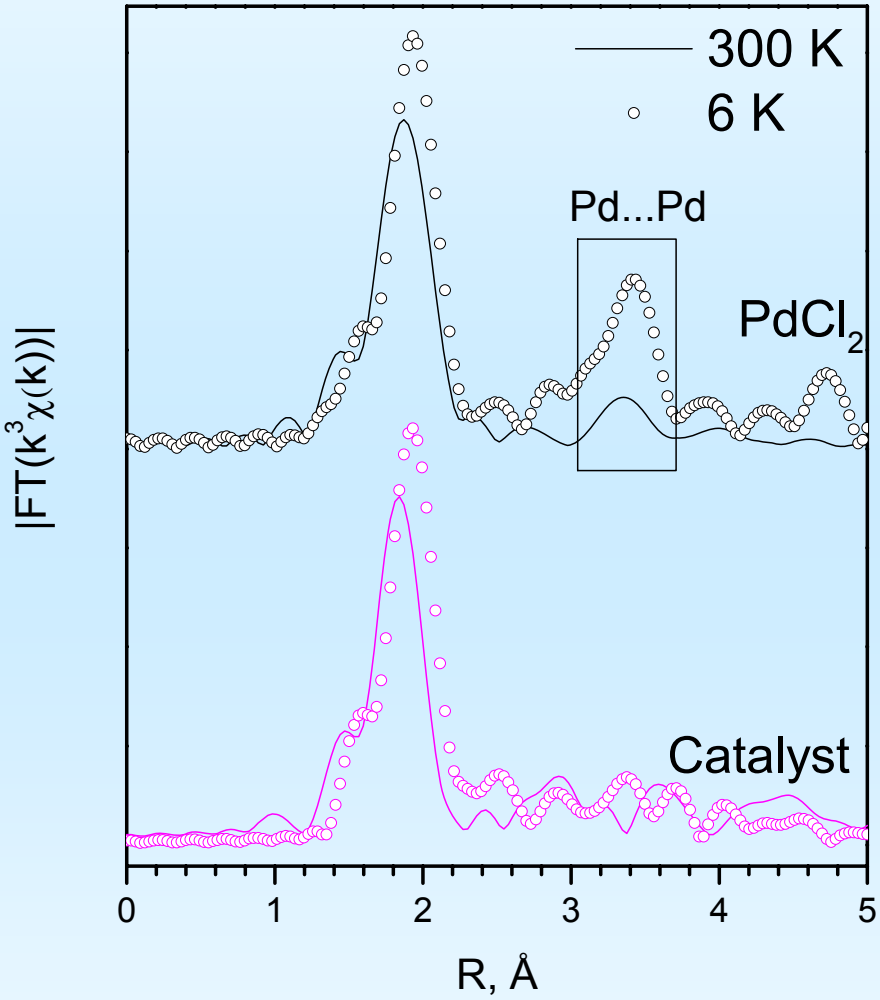

In-situ reduction of the catalyst in humid CO (at RT): Pd K-edge XANES

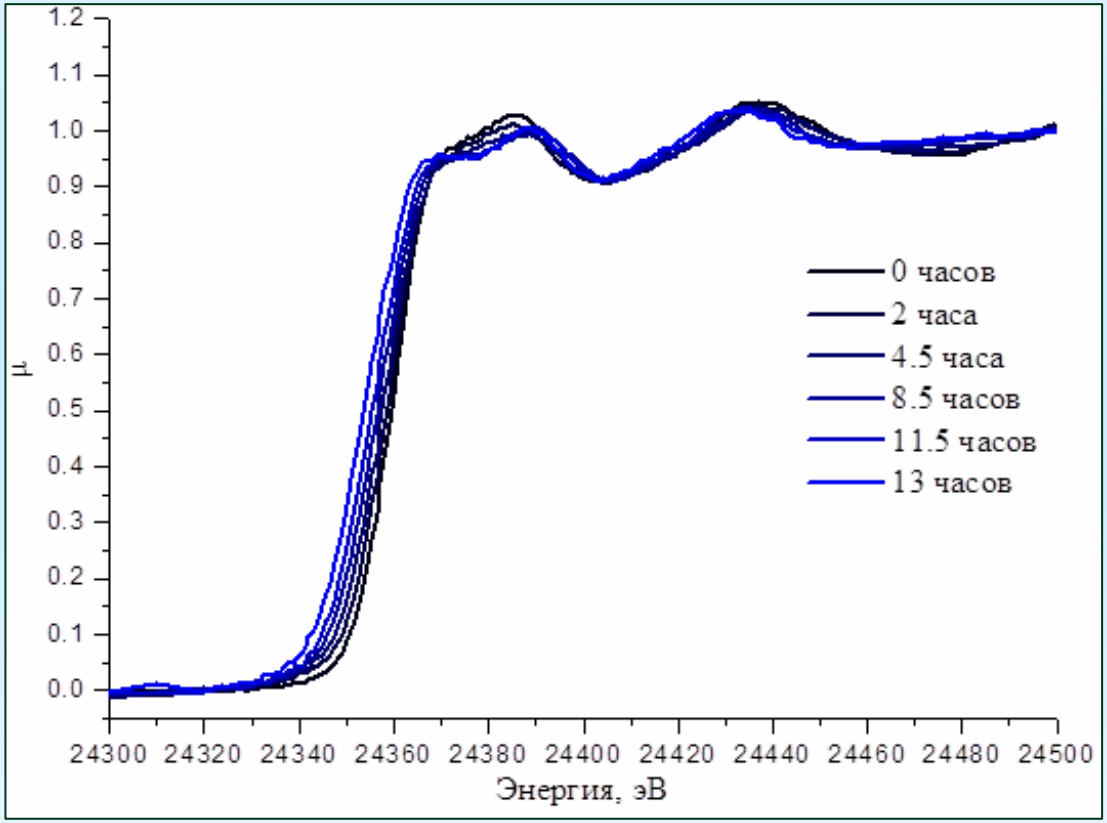

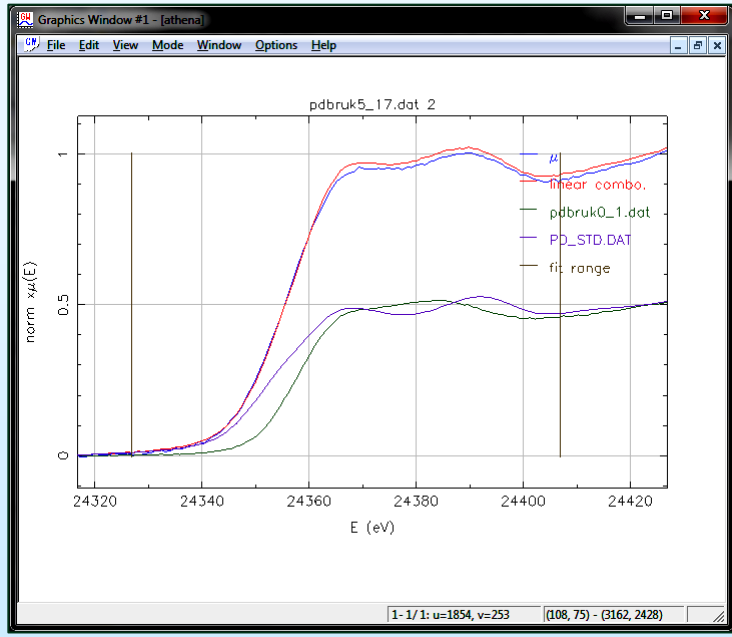

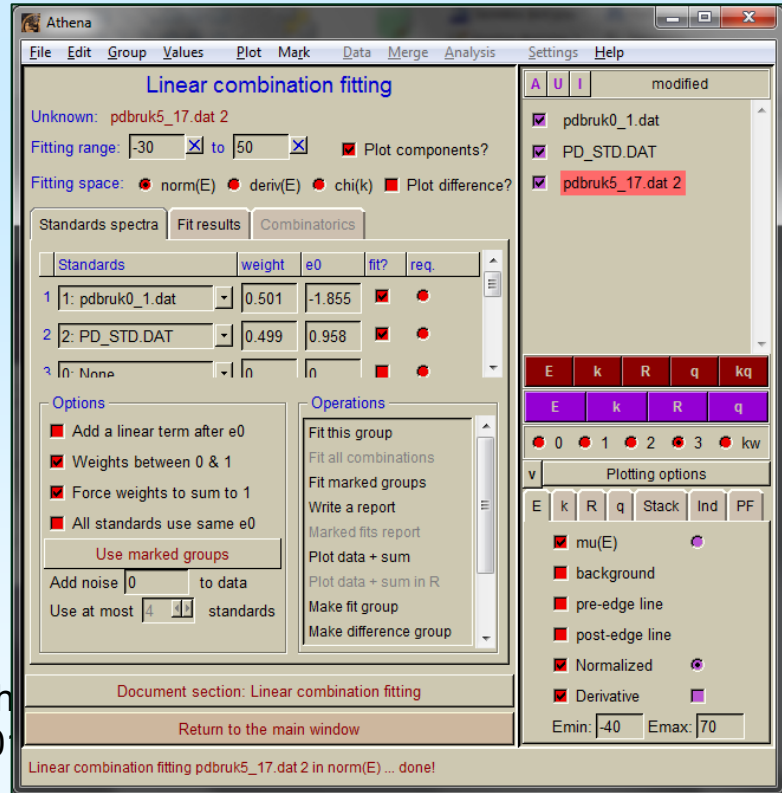

Molecular Aspects of Electroch
Dubna, 26-31 August 20

In-situ reduction of the catalyst in humid CO (at RT): Pd K-edge EXAFS

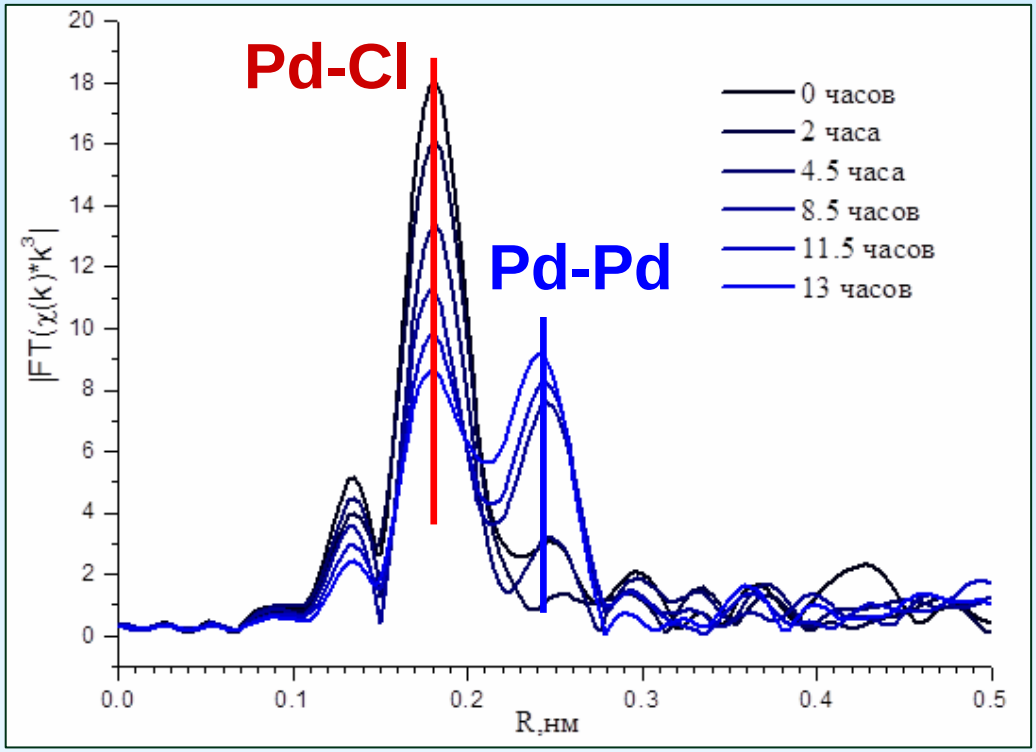

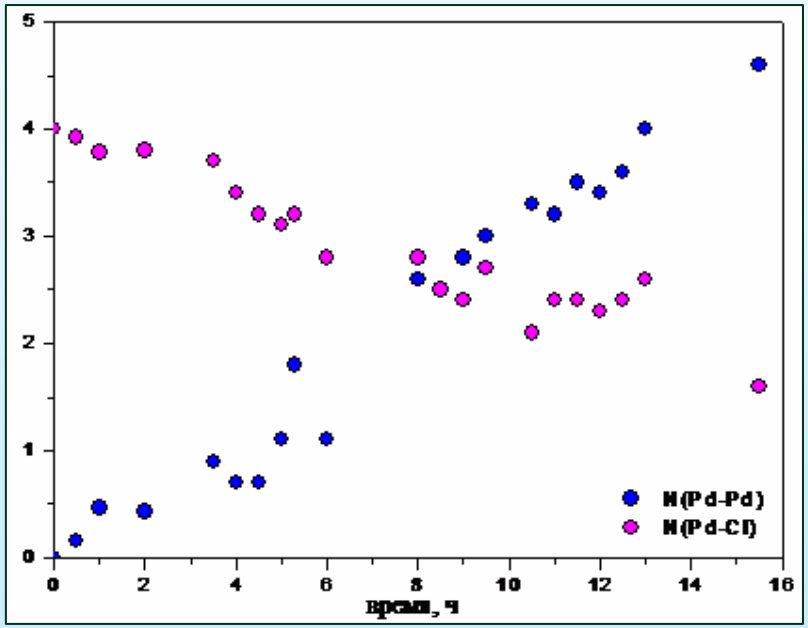

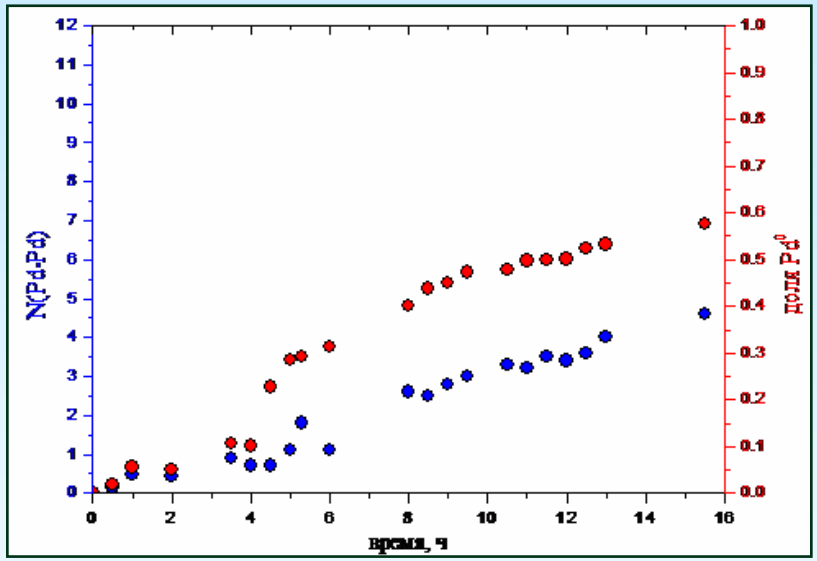

In-situ reduction of the catalyst in humid CO (at RT): XRD

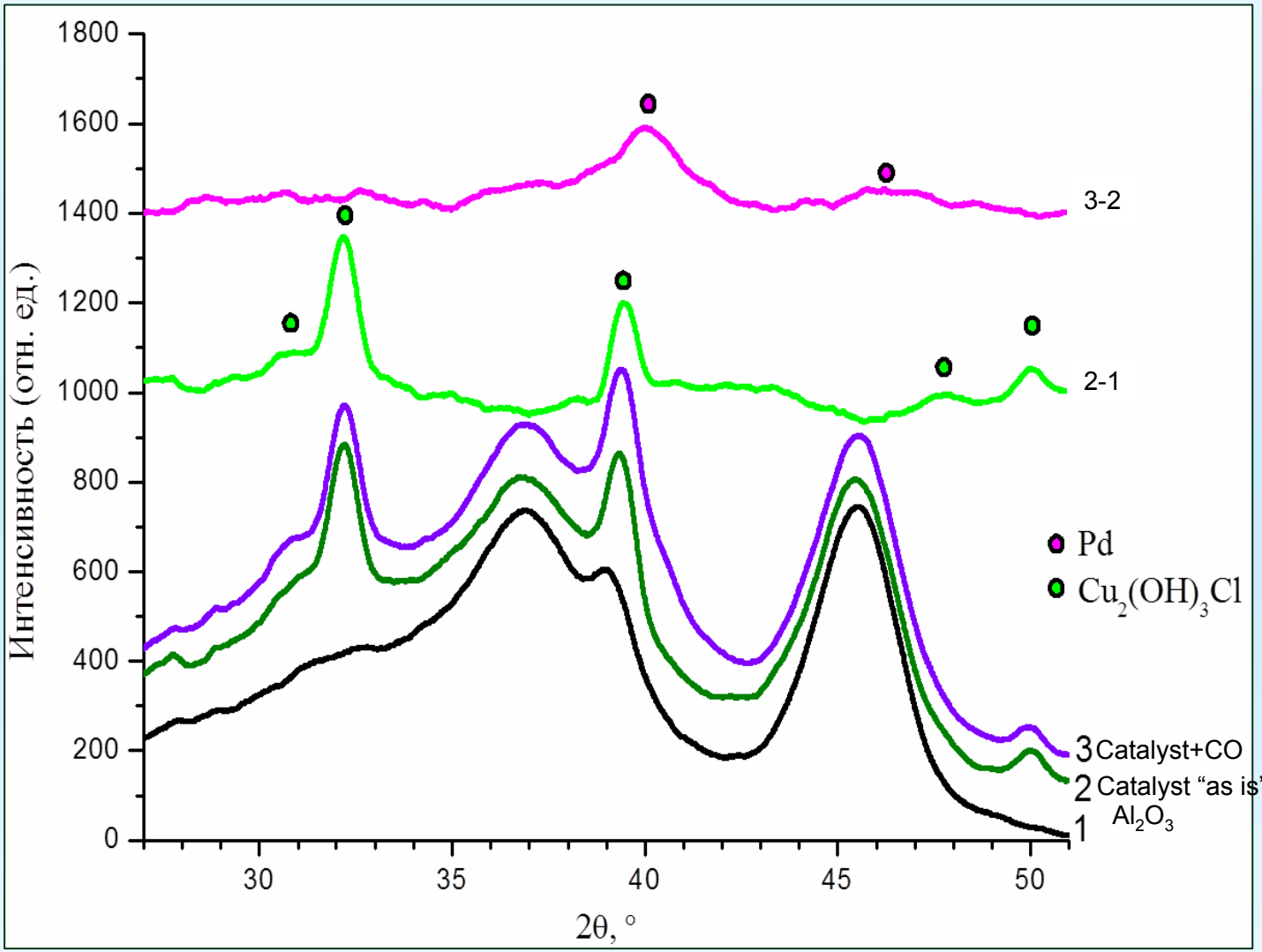

In-situ reduction of the catalyst in humid CO (at RT): Cu K-edge XANES and EXAFS

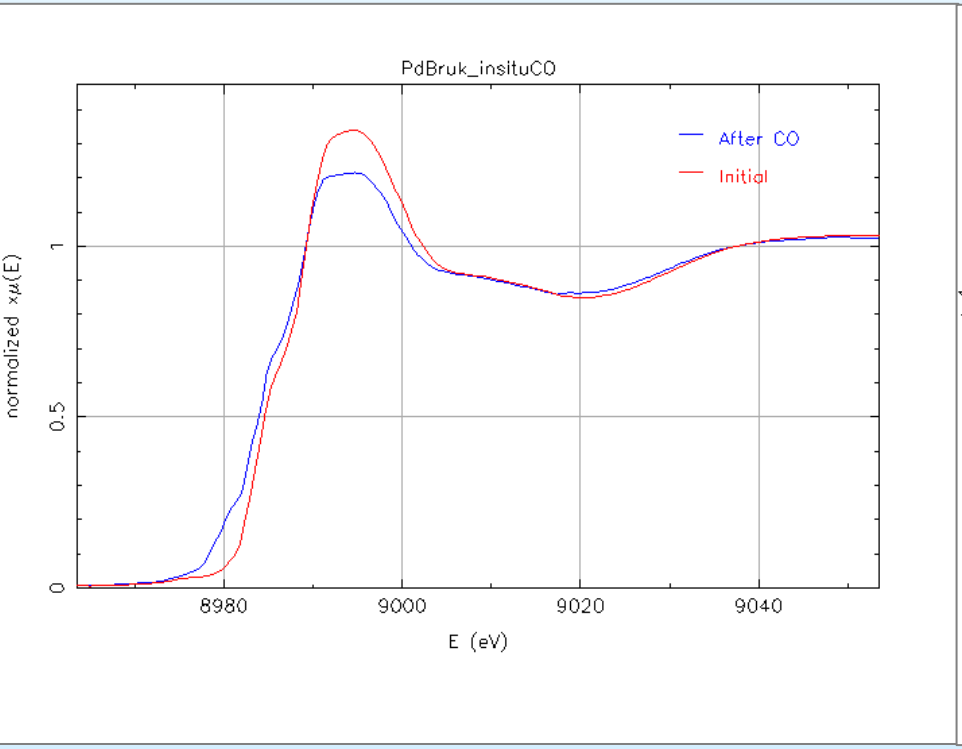

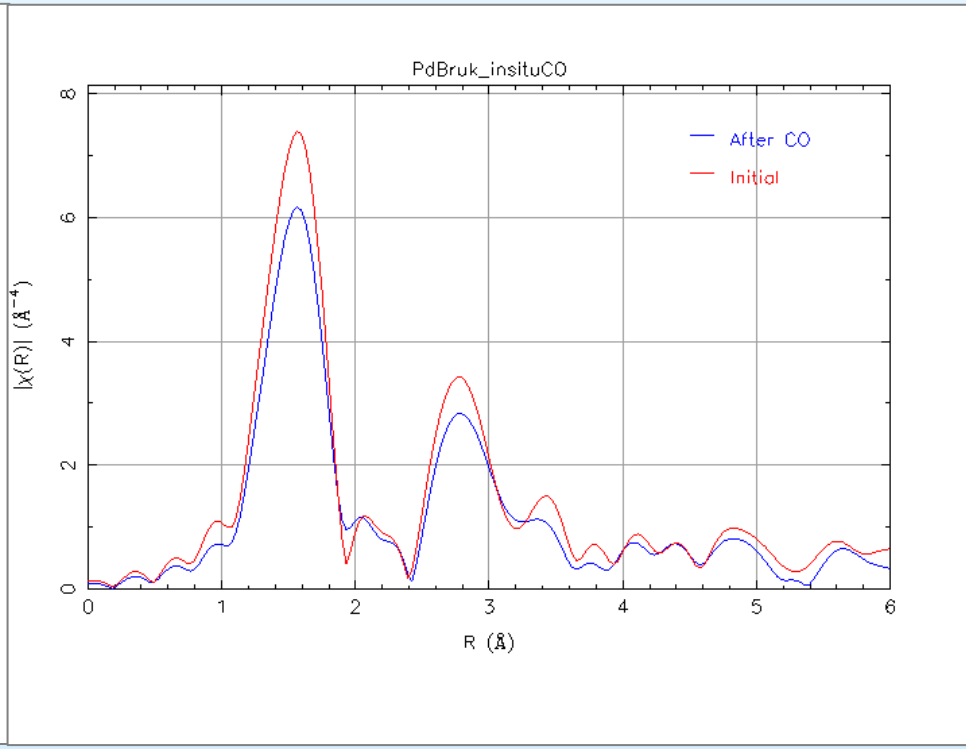

Only 10-15% of copper in the catalyst undergoes chemical modification $Cu^{2+} \rightarrow Cu^{+}$ (spatial proximity effect of Pd)

Activated Al for the small-scale hydrogen energetics

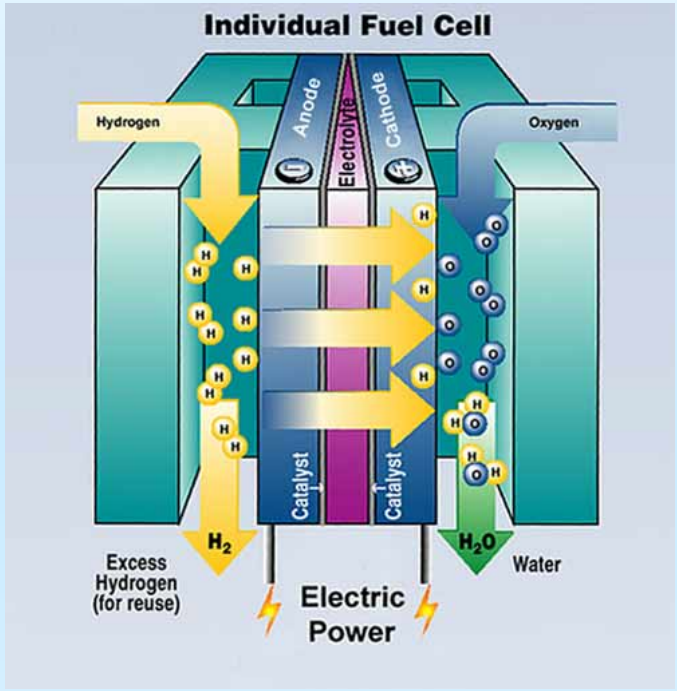

Al (any industrial alloy) $\xrightarrow{Ga_{85}In_{15}\text{-eutectics}}$ **Al**^{act} $\xrightarrow{H_2O\ (RT,\ no\ promotors)}$ $AlOOH/Al(OH)_3 + H_2$

Diffraction data

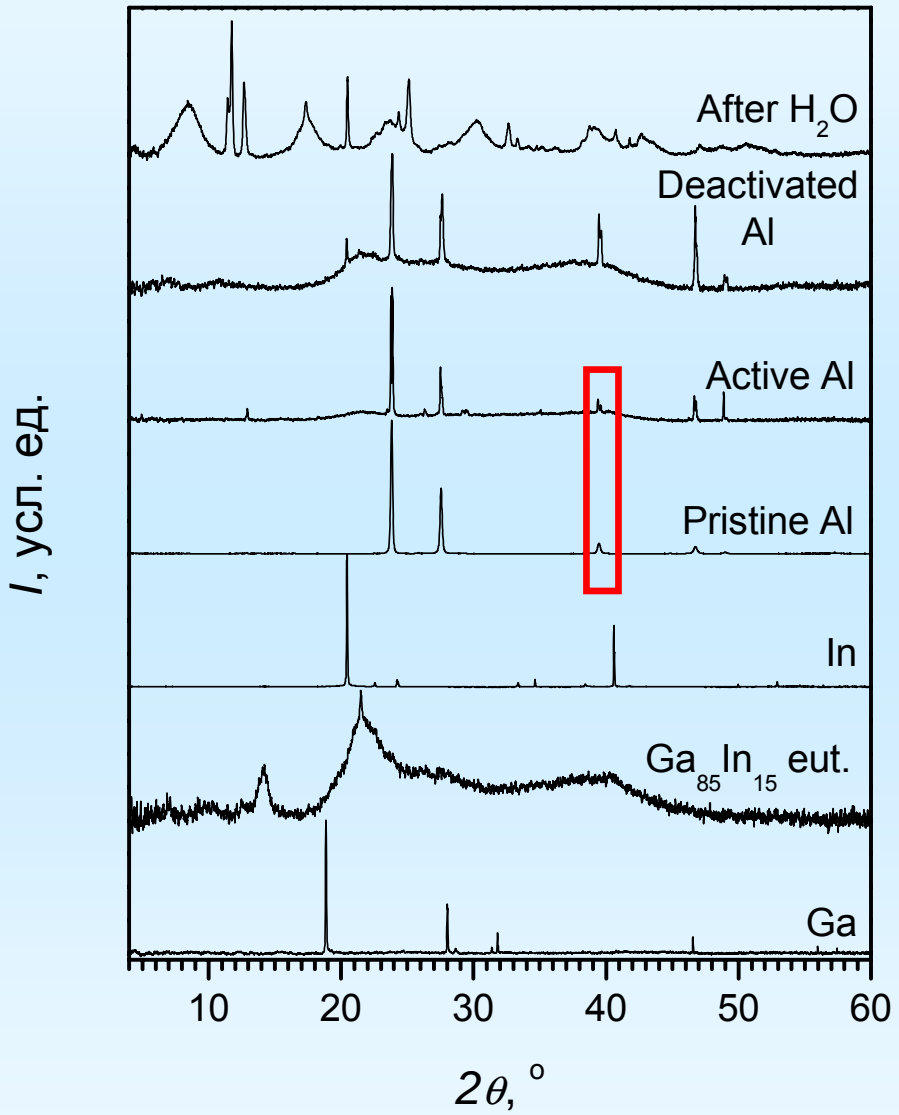

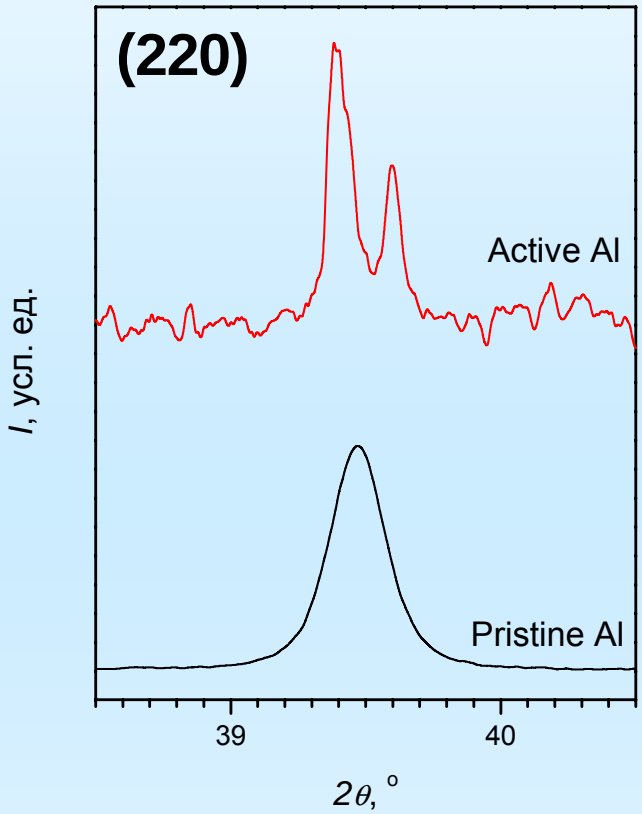

Ga K-edge XANES/EXAFS data

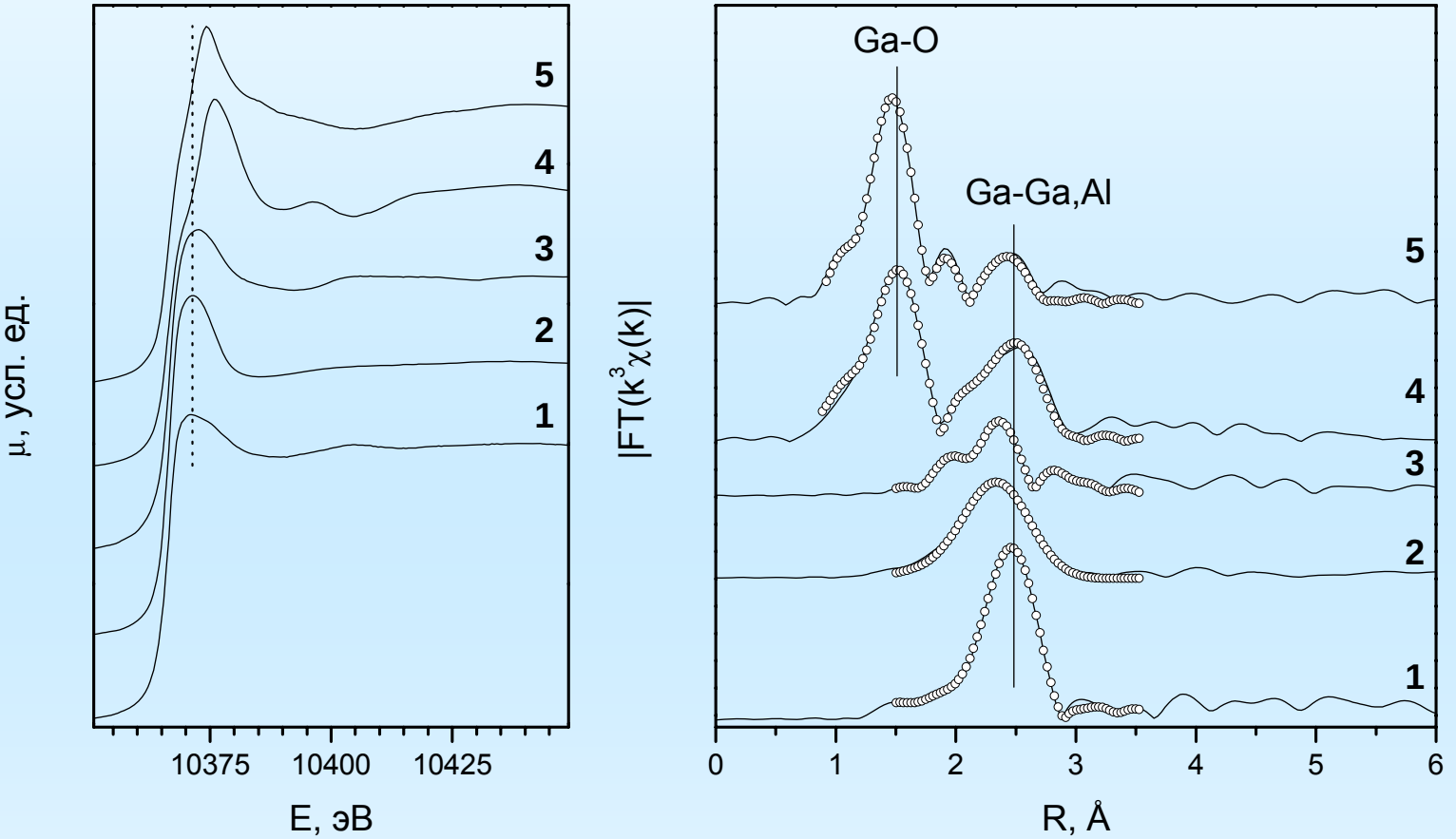

1 – Ga foil, 2 – Ga-In eutectic alloy, 3 – activated Al, 4 - active Al after H_2O, 5 – deactivated A

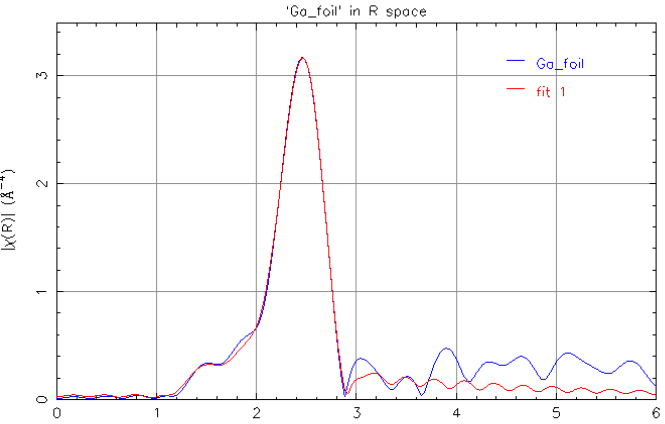

Ga foil:

N	sphere	R	σ^2
1	Ga-Ga	2.51	
4	Ga-Ga	2.68	0.0097
2	Ga-Ga	2.80	

Wavelet maps

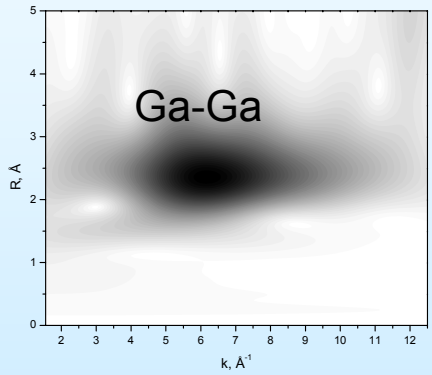

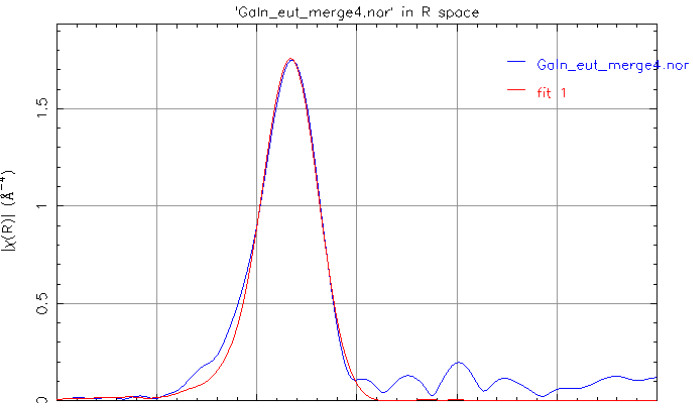

Ga-In eutectics:

N	sphere	R	σ^2
1.7	Ga-Ga	2.68	0.0026

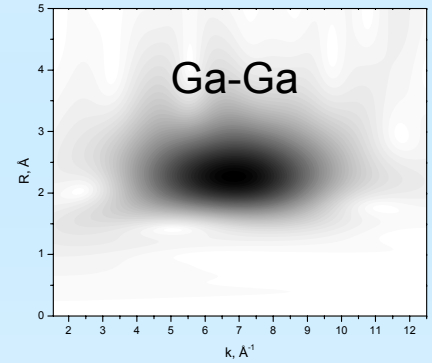

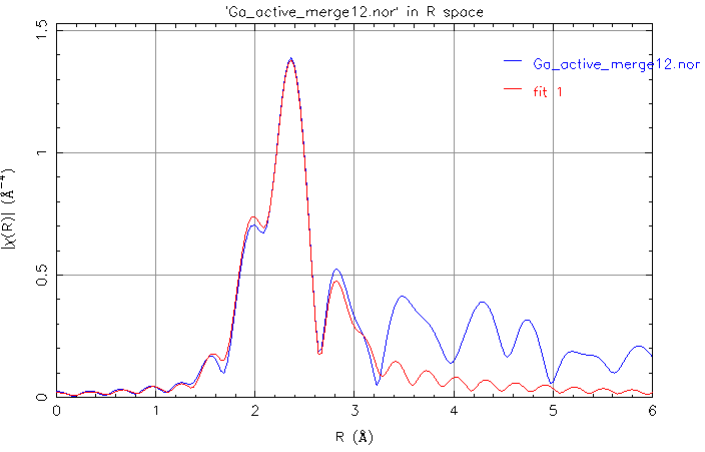

Active Al:

N	sphere	R	σ^2
1.7	Ga-Ga	2.70	0.0026
1.2	Ga-Al	2.80	0.0011

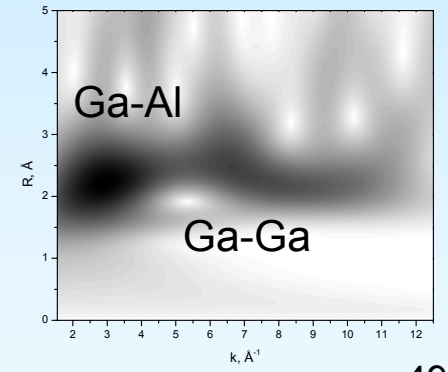

Imaging (X-ray microscopy + tomography)

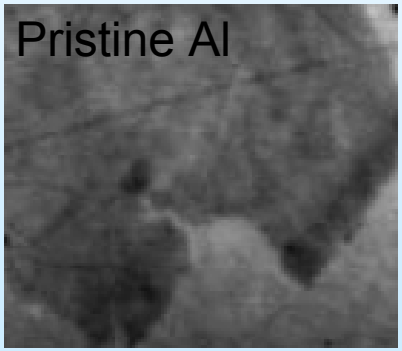

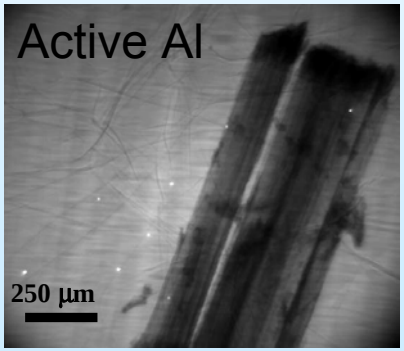

Cross-section corresponding to the geometrical centre of the sample

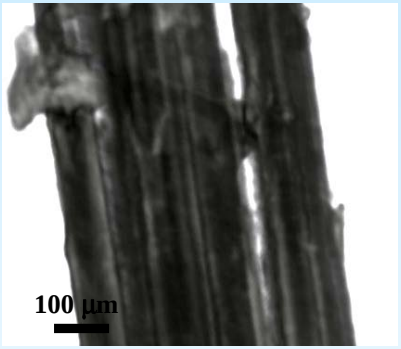

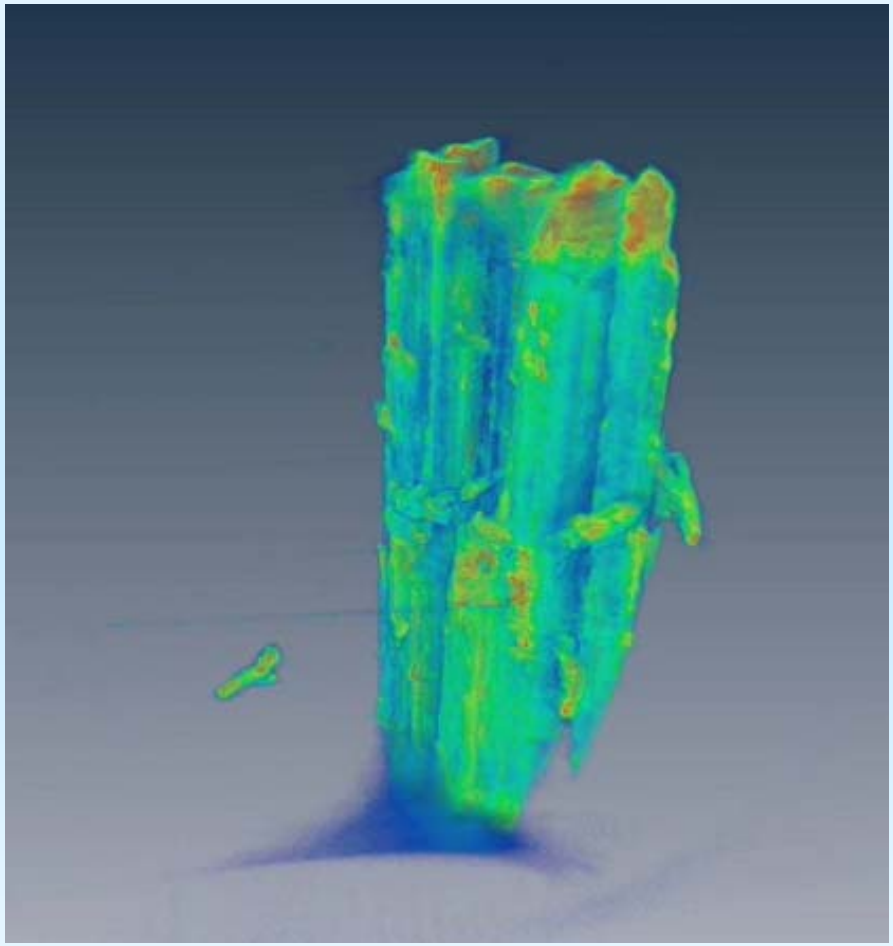

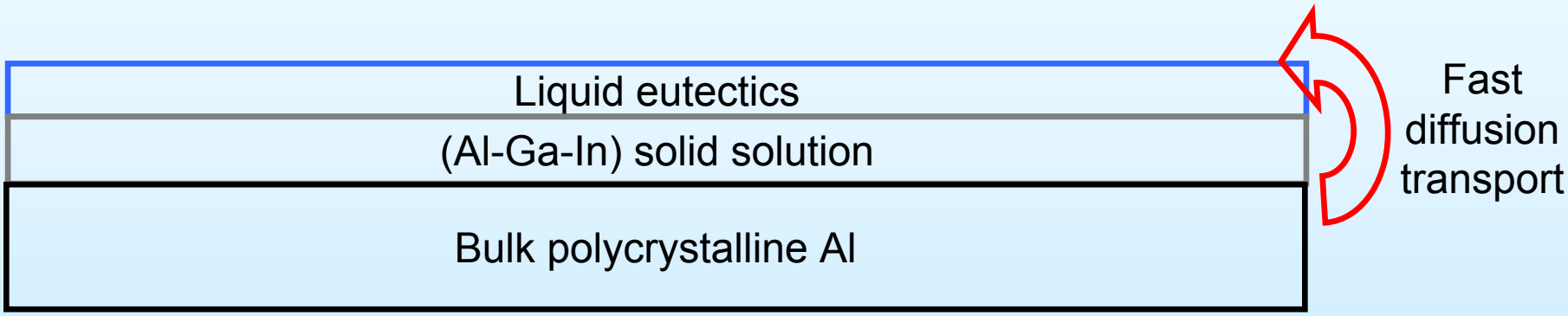

Activation mechanism: bulk diffusion of GaIn-eutectics along intergrain boundaries promoted by the emergence of (Al-Ga-In) solid solution in the subsurface layers of Al crystallites

Deactivation mechanism: decomposition of the eutectic alloy giving rise to a partial oxidation of Ga and crystallisation of In

Conclusions

- Синхротронное излучение – мощный инструмент структурной диагностики сложных слабоупорядоченных материалов
- Станция «Структурное материаловедение» в числе других станций КИСИ готова к проведению рутинных исследований (и обладает уникальными в масштабах России опытом и техническими возможностями)
- Мы открыты к сотрудничеству с любыми группами как в вопросах проведения измерений, так и реализации новых методик / модернизации оборудования

Laboratory for structural studies of non-crystalline materials, Kurchatov NBICS center, NRC «Kurchatov Institute»: Olga Beliakova, Aleksey Veligzhanin, Elena Guseva, Vadim Murzin, Evgeniy Khramov, Alfred Chernyshov, Aleksandra Shulenina

Thanks for your attention!